

**INSURANCE OF DAMAGE BY IMPORTERS**

25

**RADIO CORPORATION OF AMERICA**

75

•

## FOREWORD

This report was prepared by Radio Corporation of America under NASA Contract No. NAS 5-9131. It is a final report that covers research work conducted from January 7, 1964 to April 21, 1966, in the Electronics Research Laboratory, W. M. Webster, Director. The Project Supervisor was P. Rappaport and the Project Scientist was B. Goldstein. Some of the work on high-temperature annealing was performed by Dr. G. J. Brucker and Mr. W. Dennehy of the Physical Research Group of RCA's Astro-Electronics Division under the supervision of Dr. A. G. Holmes-Siedle.

The manuscript of this report was submitted by the authors on May 12, 1966.

## ABSTRACT

Solar cells made from silicon in which the major dopant is lithium exhibit a markedly increased radiation resistance in two forms: The first is a recovery of the solar cell in a matter of hours, after the cessation of the electron irradiation. The second is a much slower degradation rate when the irradiation flux rate is sufficiently low. In both cases, the lithium-containing cells show a performance superior to the currently used n/p cells. This radiation-resistant behavior holds true for parameters such as  $P_{\max}$ ,  $I_{sc}$ , minority carrier diffusion length  $L$ , and spectral response, and for both 1-MeV electron and 16.8-MeV proton irradiations. The recovery rate after a 1-MeV electron irradiation has a time constant of approximately 1 hour, and the ratio of its values at 30°C and 0°C is the same as the inverse of the lithium diffusion coefficient. Our (preliminary) speculation is that the lack of damage in the recovered solar cell is due to the preferential formation of a new damage center (over, for example, the A- and E-center) due to lithium migration, and the fact that these new centers (L-centers, see below) do not degrade the lifetime appreciably.

Electron paramagnetic resonance studies have been made of the interaction between lithium and electron-irradiation defects in n- and p-type silicon, and in silicon in which lithium is the predominant impurity. In n-type silicon, the presence of lithium decreases the A-center EPR absorption and, conversely, the presence of A-centers decreases the lithium EPR absorption. It has been shown that this interaction is not merely a donor electron transfer from lithium to A-center but, rather, a more direct atomic interaction. In p-type silicon, the presence of lithium does not significantly affect the EPR absorption due to the K-center, the dominant (paramagnetic) damage center found in p-type material.

In silicon in which lithium is the predominant impurity, lithium-defect interactions have been observed directly. A new paramagnetic center is observed, but *only* when both lithium and damage centers are present. This new center, called the L-center, has no discernible angular dependence and has a g-value of  $1.9996 \pm 0.0005$  at 27°K. It has an apparent introduction rate of about 0.3 to 0.5  $\text{cm}^{-1}$  and involves neither phosphorus nor oxygen. It appears to be a shallow level ( $\approx 0.03$  to 0.05 eV below the conduction band), which would suggest that it is not an effective recombination level for minority carriers, namely holes.

We have studied the paramagnetic properties and growth of the K-center, the dominant defect introduced into p-type silicon by electron irradiation, as functions of resistivity, impurity dopants, and illumination. The defect has a spin of 1/2 and has g-values of 2.0000, 2.0066, and 2.0056 in which the principal magnetic axes lie along the  $\langle 221 \rangle$ ,  $\langle 1\bar{1}0 \rangle$ , and  $\langle 11\bar{4} \rangle$  crystallographic directions, respectively. No hyperfine interactions are observed. The introduction rates for the K-center are 0.006, 0.025, 0.073, and 0.11  $\text{cm}^{-1}$  at bombardment energies of 0.7, 1, 3, and 6.6 MeV, respectively. The K-center is independent of the p-type dopant. It is not a primary defect, but requires oxygen. We have associated the K-center with a previously reported 0.3-eV defect level because both require oxygen, both have about the same introduction rates and bombardment energy dependence, and the value of the Fermi level at which the K-center EPR absorption decreases sharply is about 0.3 eV. Preliminary measurements have indicated a reverse-annealing at about 250°C, followed by normal annealing of the damage to very low levels by about 450°C. A physical model for the K-center is offered in terms of a complex of two vacancies and two oxygen atoms which have trapped a hole.

# TABLE OF CONTENTS

| <i>Section</i>   | <i>Page</i> |
|--|-------------|
| I. ELECTRICAL AND EPR STUDIES OF THE K-CENTER IN p-TYPE SILICON .....  | 1           |
| A. Summary of Experimental Results .....   | 1           |
| B. Model of the K-Center .....   | 2           |
| C. High-Temperature Annealing of the K-Center .....  | 4           |
| 1. Introduction .....  | 4           |
| 2. Results .....   | 4           |
| 3. Discussion .....  | 6           |
| II. STUDIES OF LITHIUM-DEFECT INTERACTIONS BY EPR MEASUREMENTS .....   | 7           |
| A. Summary of Effects of Lithium in Phosphorus-Doped (n-type) Silicon and Boron-Doped (p-type) Silicon ..... | 7           |
| B. Silicon Doped Predominantly with Lithium .....  | 7           |
| C. Discussion .....  | 11          |
| III. INCREASED RADIATION RESISTANCE OF SOLAR CELLS THROUGH THE USE OF LITHIUM .....                          | 14          |
| A. Introduction.....   | 14          |
| B. Experimental Details of the Lithium Study .....   | 14          |
| C. n/p Solar Cells .....   | 15          |
| D. p/n Solar Cells .....   | 16          |
| 1. Electron Irradiations .....   | 16          |
| 2. Proton Irradiations .....   | 28          |
| 3. Gamma Irradiations .....  | 31          |
| E. Discussion .....  | 31          |
| IV. SUMMARY OF CONCLUSIONS AND RECOMMENDATIONS FOR FUTURE WORK .....   | 34          |
| A. The K-Center .....  | 34          |
| B. Lithium-Defect Interactions .....   | 34          |
| 1. EPR Studies .....   | 34          |
| 2. Increased Radiation Resistance of Solar Cells .....   | 35          |
| REFERENCES .....   | 36          |

## ILLUSTRATIONS

| <i>Figure</i>   | <i>Page</i> |
|---|-------------|
| 1. Silicon unit cell .....  | 2           |
| 2. Suggested model for the K-Center .....   | 3           |
| 3. g-Values of the K-Center lines .....   | 5           |
| 4. Basic results of the EPR measurements .....  | 5           |
| 5. Resonance lines as a function of microwave power .....   | 6           |
| 6. Significant EPR results .....  | 9           |
| 7. Effects of high oxygen concentration and of bombardment flux level on the Li paramagnetic resonance .....                              | 10          |
| 8. EPR data for the phosphorus doublet lines, the resonance line due to lithium alone, and the new L-Center line at different times ..... | 12          |
| 9. Typical L vs. $\phi$ characteristic of n/p floating-zone cells .....   | 16          |
| 10. Result of irradiation of Li-diffused F.Z. cells .....   | 18          |
| 11. Annealing behavior of Li-diffused F.Z. cells .....  | 18          |
| 12. Behavior of L vs. $\phi$ in a lithium-doped cell and a standard cell .....  | 19          |
| 13. Adjusted plot of L vs. $\phi$ (Figure 12) .....   | 20          |
| 14. Recovery of L at room temperature for two fluxes .....  | 21          |
| 15. Effect of temperature on the recovery .....   | 22          |
| 16. $(L-L_0)/(L_{AB}-L_0)$ plotted on semilog scale .....   | 22          |
| 17. Short-circuit current as a function of irradiation .....  | 23          |
| 18. Maximum power output as a function of irradiation .....   | 24          |
| 19. Maximum power output as a function of flux .....  | 24          |
| 20. Spectral response of 1-cm $\times$ 2-cm solar cell (LiCS SiO-586) .....   | 25          |
| 21. Spectral response of 1-cm $\times$ 2-cm solar cell (BoFH 9 p/n) .....   | 26          |
| 22. Fraction of remaining damage (f) as a function of temperature .....   | 27          |
| 23. Short-circuit current as a function of temperature .....  | 27          |
| 24. Isothermal annealing measurements .....   | 28          |
| 25. $I_{sc}$ as a function of flux of 16-MeV protons .....  | 29          |
| 26. $P_{max}$ as a function of flux of 16.8-MeV protons .....   | 30          |
| 27. Fractional change in current vs. gamma dose .....   | 30          |

# I. ELECTRICAL AND EPR STUDIES OF THE K-CENTER IN p-TYPE SILICON

## A. SUMMARY OF EXPERIMENTAL RESULTS

The studies of the EPR and electrical properties of the K-center have been completed. We have found that the K-center is the predominant paramagnetic defect introduced into p-type silicon by electron bombardment at energies ranging from 0.7 to 6.6 MeV. Its net electron spin is  $1/2$ . Its g-values are 2.0000, 2.0066, and 2.0056 for the  $\langle 221 \rangle$ ,  $\langle 1\bar{1}0 \rangle$ , and  $\langle 11\bar{4} \rangle$  directions, respectively. The K-center is not a primary defect but requires oxygen, suggesting that atomic motion of either (interstitial) silicon and/or oxygen may be involved. From EPR measurements, we could not determine the bonding arrangement and the physical structure of the defect because of the lack of hyperfine structure in the spectrum.

The formation of the K-center is independent of the p-type dopant. Its introduction rates at 0.7, 1, 3, and 6.6 MeV are, respectively, 0.006, 0.025, 0.073, and  $0.11 \text{ cm}^{-1}$ . At high fluxes, depending in part on bombardment energy and in part on the starting resistivity, the EPR measured K-center concentration decreases. However, subsequent illumination experiments and annealing experiments show that the defects are still present, but of different electronic charge state because they have trapped an electron.

This decrease in the K-center concentration with flux has been shown to be dependent on the Fermi level position from spin resonance and resistivity measurements. From these investigations, the K-center, which acts as a hole trap, is identified with the 0.3-eV defect level. This is based on the following of our measurements: Both have the same introduction rate and energy dependence for their formation, and both require oxygen. Hall measurements show the presence of the 0.3-eV defect level only when the K-center EPR spectrum is observed. Finally, the K-center EPR absorption decreases sharply as the Fermi level, moving away from the valence band, passes through a value of about 0.3 eV.

The identification of the K-center with the 0.3-eV level is supported by the results of photoconductivity investigations of Vavilov et al.,<sup>1</sup> and by the optical absorption studies of Fan and Ramdas.<sup>2</sup> They also find that in order to detect the  $4\text{-}\mu$  band (0.3 eV) in p-type silicon the Fermi level must lie below it. Furthermore, the heat-treatment studies of the  $4\text{-}\mu$  band by Fan and Ramdas are in agreement with our results. That is, on samples for which  $E_F$  after bombardment is greater than 0.3 eV, the K-center and  $4\text{-}\mu$  band are not detected, and after heat treatment they are observed.

The fact that oxygen is required for the formation of the K-center (the 0.3-eV level) suggests that it is not a primary defect created by the bombardment. Motion of primary defects at high temperature has been established by Watkins.<sup>3</sup> The K-center is probably the result of the migration of one of these defects and the subsequent interaction, when it is sufficiently close, with oxygen, either in an intermediate or final step of the process, which produces the K-center. It appears likely that, of the several primary defects created in silicon, the isolated lattice vacancy, which is less stable than the divacancy (but has a higher introduction rate), is involved in the formation of the K-center. In this connection, Vavilov et al.<sup>1</sup> have demonstrated that the

0.3-eV defect level in p-type silicon is not immediately formed by electron irradiation. In their photoconductivity experiments, samples were irradiated and measured at 100°K. They observe that only after the temperature has been raised to  $\approx 300^\circ\text{K}$  for 16 hours does a 0.3-eV photoconductive band appear. These authors also associate the 0.3-eV level with oxygen.<sup>1</sup>

## B. MODEL OF THE K-CENTER

The experimental details of the work described above have been treated in detail in the Semiannual Report dated July 7, 1965.\* We have recently concluded some theoretical speculations and now propose and discuss briefly a physical model of the K-center. This model must be consistent with our experimental data; specifically, we must have (a) the symmetry of the g-tensor, (b) the necessity of oxygen for its creation, (c) the failure to observe hyperfine structure, and (d) the necessity for trapping a hole at the K-center in order to detect it in spin resonance measurements.

It should be noted that even when the model conforms with the above-mentioned requirements, it will not necessarily be unique because the information currently available is not sufficient to determine the structure of the defect.

To help picture the model we show first the bonding arrangement of a group of silicon atoms in the crystal, Fig. 1. The four bonds of a silicon atom lie in pairs in perpendicular (110)

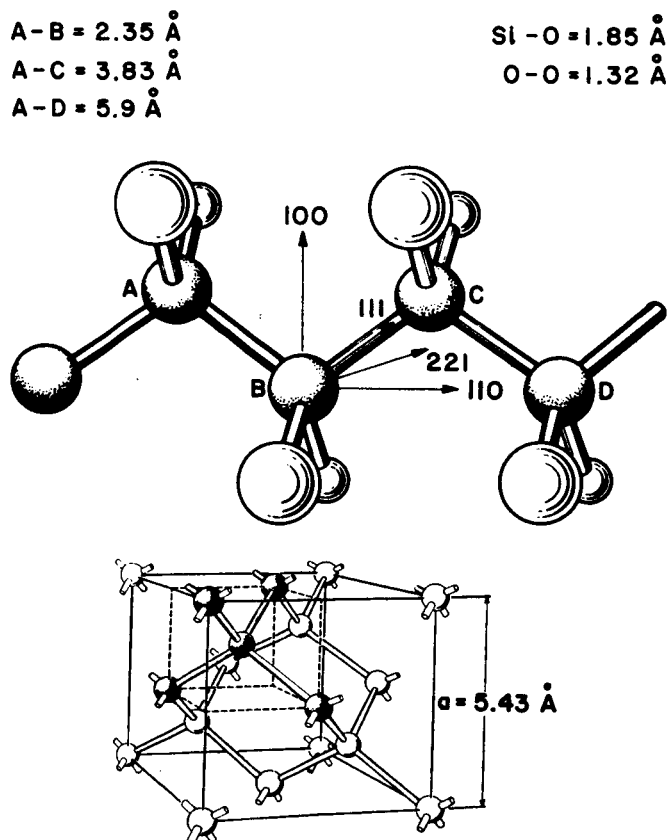


Fig. 1.  
Silicon unit cell.

\*Contract No. NAS 5-9131.

planes. (This is probably the reason why all paramagnetic defects in silicon have one of their principal *g*-axes along a  $[110]$  direction.) The numbers at the top of the figure refer to the tetrahedral bond distances between the given atoms. When oxygen is present it is normally interstitial, forming a nonlinear bond between two adjacent silicon atoms.<sup>4</sup> Infrared studies of crystals heat-treated at  $350^{\circ}\text{C}$  have shown that oxygen tends to cluster, forming  $\text{SiO}_4$  complexes in concentrations of the order of  $10^{17}/\text{cm}^3$  (Ref. 4). On this basis we have assumed that pairs of oxygen about two lattice distances apart are present with comparable densities in quartz-crucible-grown silicon without heat treatment. Specifically, we consider that one of the oxygen atoms shares its bonds with the silicon atoms A and B while the other shares with atoms C and D. The K-center is then formed when two vacancies are trapped by these oxygen atoms.<sup>3</sup> This results in the structure shown in Fig. 2. We can visualize the construction of the defect as follows: Initially, an A-center is formed when one vacancy is trapped (say at atom C) by one of the oxygen atoms. Capture of a second vacancy (at atom B) does not form two separate A-centers but rather the K-center, because the oxygen atoms are sharing a common bond.

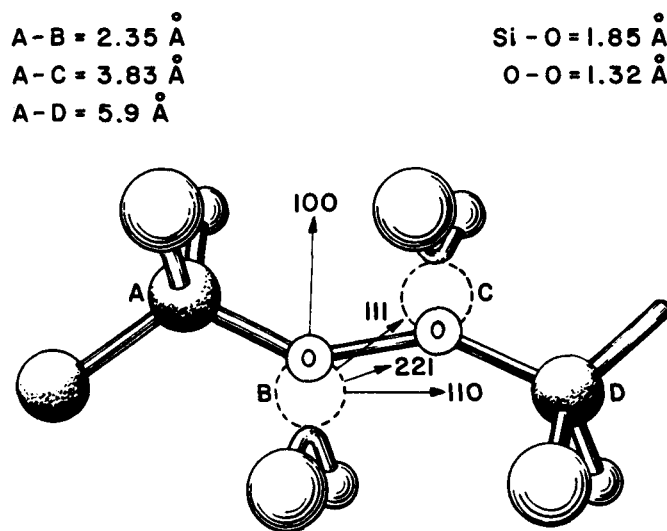


Fig. 2. Suggested model for the K-Center.

The state shown in Fig. 2 is overall neutral. The system is under strain because the combined tetrahedral bond distances of Si-O and O-O are smaller by  $1 \text{ \AA}$  than the distance between atoms A and D. The strain can be relieved if a hole is trapped at the O-O bond. A loosely bound unpaired electron in this bond would then be responsible for the observed spin resonance signal.

This model satisfies our experimental results. First, the axially symmetric axis of the K-center is the  $\langle 221 \rangle$ , which is expected to lie along the bond axis.<sup>5</sup> The model in Fig. 2 shows that the O-O axis is in this direction. Second, the requirement of oxygen is met. Third, the lack of hyperfine structure is accounted for because of the small concentrations of oxygen (0.04%) which have a nuclear spin different from zero. (Contributions to the hyperfine structure from next-nearest-neighbor  $\text{Si}^{29}$  atoms are usually quite small.) Finally, it requires the trapping of a hole to be observed in spin resonance as was discussed in the preceding paragraph.



## C. HIGH-TEMPERATURE ANNEALING OF THE K-CENTER

### 1. Introduction

High-temperature annealing studies of the K-center were undertaken to extend the annealing work carried out earlier in the contract period. The temperature range was that used by Fang,<sup>6</sup> so that his electrical measurements could be correlated with the EPR studies of the K-center annealing properties described below.

Isochronal annealing studies (20-min. duration) of the K-center were carried out with samples of p-type, boron-doped, pulled silicon. The sample dimensions were 0.1 in.  $\times$  0.3 in.  $\times$  0.035 in. with the largest face being the (001) plane. The K-centers were produced by a 1-MeV electron beam current of  $2.5 \mu\text{A}/\text{cm}^2$ , and the samples were irradiated with the beam normal to the (001) plane. The temperature of the samples during bombardment was  $40^\circ\text{C}$ .

Three identical samples were used for the final isochronal annealing studies. Their original resistivity was  $0.6 \Omega\text{-cm}$ ; after bombardment by a flux of  $6 \times 10^{17}/\text{cm}^2$ , the resistivity was  $2.7 \Omega\text{-cm}$ . One sample was maintained as a control unit. The second and third were initially annealed at  $100^\circ\text{C}$  and  $200^\circ\text{C}$ . After this temperature of  $200^\circ\text{C}$  was reached, the second sample was heated in a separate oven at  $200^\circ\text{C}$  each time the third (the actual measurement sample) was annealed at higher temperatures. The purpose of this procedure was to determine if there was any K-center annealing time-dependence at temperatures over  $200^\circ\text{C}$ , since the initial experiments indicated reverse K-center annealing at temperatures over  $200^\circ\text{C}$ . The annealing was carried out in a forming gas ambient. Temperatures were measured by means of a thermocouple located in the sample boat and were maintained within  $\pm 3^\circ\text{C}$ . All K-center EPR measurements were made in the absorption mode at liquid-neon temperature ( $27^\circ\text{K}$ ) with a Varian 9-GHz EPR spectrometer which has been previously described.<sup>7</sup> Calibration of the spectrometer was achieved by including a known phosphorus-doped silicon sample along with the irradiated silicon samples for each measurement, and the results were normalized to equal phosphorus-doublet signal. Sample resistivity was measured after each heat treatment with a four-point probe.

### 2. Results

A typical EPR spectrum of the K-center is shown in Fig. 3. The phosphorus-doublet signals are separated by about 40 gauss and the K-center lines are located between them. The silicon samples were oriented so that the magnetic field was perpendicular to the (001) plane. This has been shown to give a two-line spectrum.<sup>7</sup> Magnetic field markers were recorded on each spectral run and the spectrometer frequency measured. The g-values of the K-center lines were calculated from these data and are given in Fig. 3.

The basic results of the EPR measurements are shown in Fig. 4. The unannealed fraction versus temperature for both K-center density and resistivity are plotted together. The peak heights of both spin resonance lines were added together and it is the total height which is plotted. The validity of this technique for measuring relative spin densities has been discussed by Corbett and Watkins.<sup>8</sup> The control sample indicated that there was no time dependence for K-center annealing at  $200^\circ\text{C}$ .

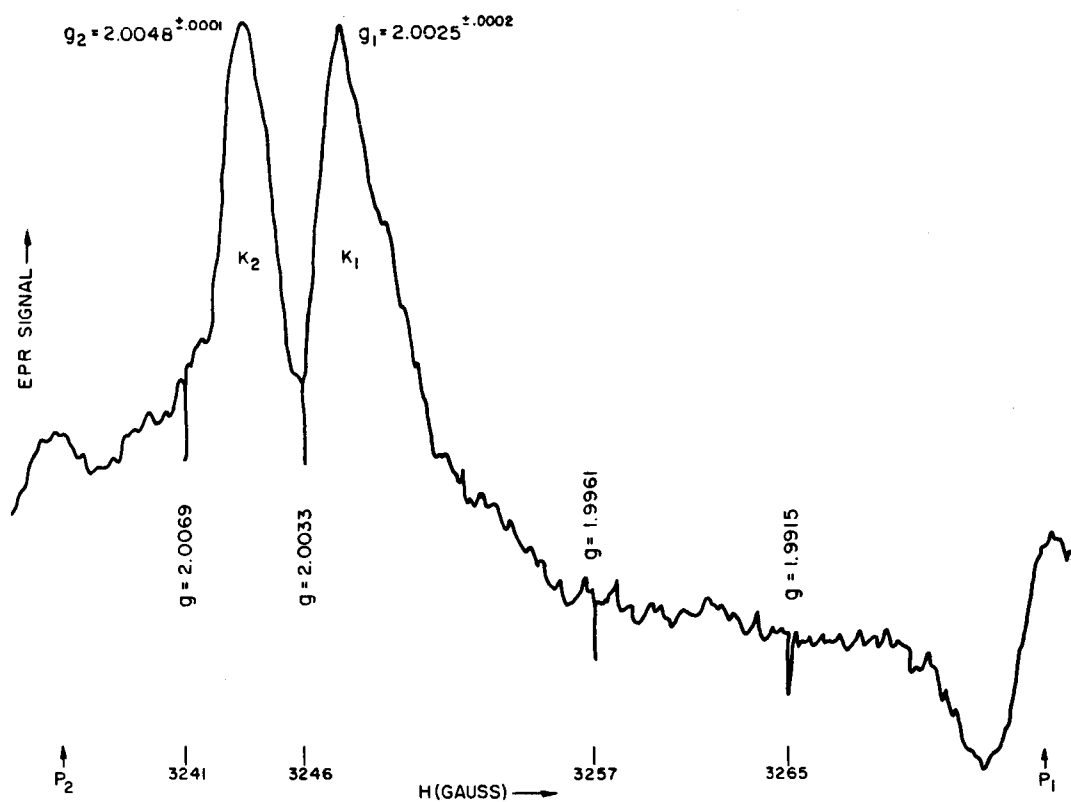


Fig. 3. g-Values of the K-Center lines.

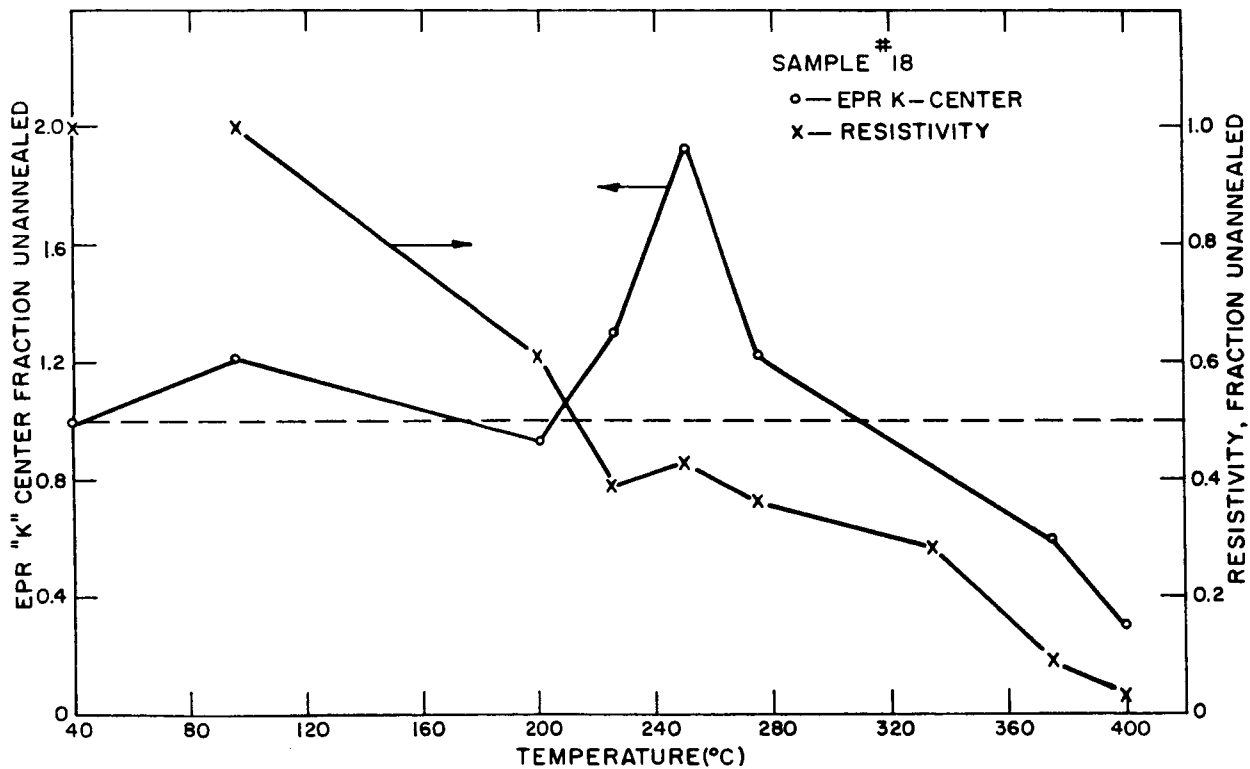


Fig. 4. Basic results of the EPR measurements.

### 3. Discussion

The increase in signal due to annealing at temperatures of about 250°C is a most interesting result. Both controls behaved well and no unusual changes in the operation of the machine were observed. Resistivity continued to decrease in this temperature region and showed a slight increase at the temperature where the maximum of the EPR signal occurred. The increase in the EPR signal at 250°C cannot be attributed to any Fermi-level shift since resistivity measurements indicated that the Fermi level was located 0.2 eV above the valence band at the start of the annealing experiment. This means that it was located below the K-center level which lies 0.3 eV above the valence band. It should be noted that the J-center anneals in the region of 200°C to 300°C. If this results in divacancy dissociation, then it could be a source of vacancies for the formation of K-centers.

Experimental evidence to support the observation of the K-center reverse annealing was obtained in a series of measurements to determine if any saturation effects could account for the EPR signal increase at 250°C. A control sample was used to obtain the dependence of the phosphorus-doublet signal and the K-center signal on microwave power transmitted to the cavity. These resonance lines are plotted versus microwave power in Fig. 5. The operating point for the annealing experiments is indicated on the curves, and it is evident that both the K-center and phosphorus signals were linearly dependent on power within a wide range around the operating point. In addition, it was established that even if we did operate in the "saturation" region, the ratio of K-center signal to phosphorus signal was constant.

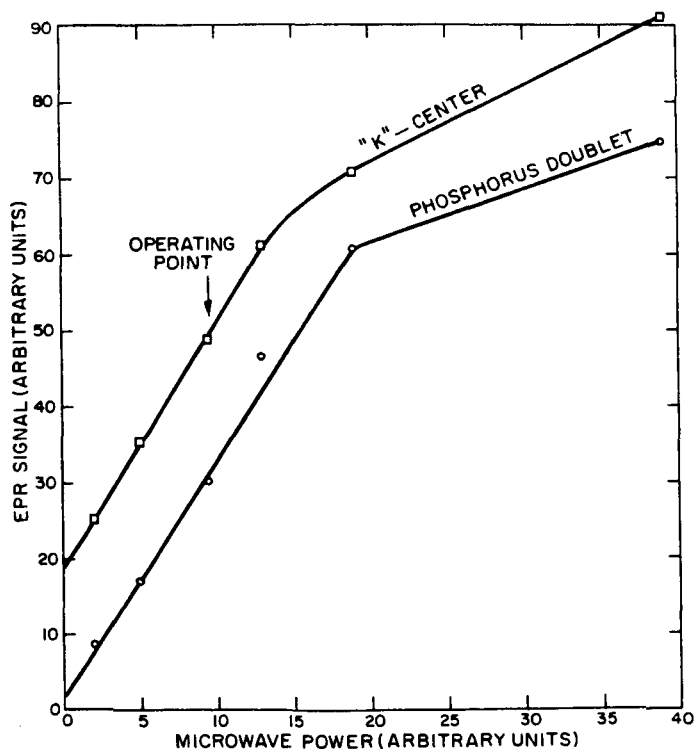


Fig. 5. Resonance lines as a function of microwave power.

## II. STUDIES OF LITHIUM-DEFECT INTERACTIONS BY EPR MEASUREMENTS

### A. SUMMARY OF EFFECTS OF LITHIUM IN PHOSPHORUS-DOPED (n-type) SILICON AND BORON-DOPED (p-type) SILICON

In n-type silicon evidence for the atomic interaction between lithium and A-centers, though indirect, is considered to be quite strong. The only evidence considered direct would be the observation of a third EPR center different from the lithium or the A-center. This third center has not been found. However, we have unambiguously shown that the presence of lithium decreases the A-center resonance line, and that the appearance of A-centers decreases the lithium resonance line. We have shown further that these effects cannot be explained merely on the basis of the transfer of valence electrons from one center to another. It is postulated, therefore, that an atomic complexing of some sort is taking place due to the high mobility of the lithium.

In p-type silicon, no indication of any Li-defect interactions is observed. The presence of lithium does not significantly change the density, g-value, or gross angular dependence of the dominant damage defect, the K-center.

### B. SILICON DOPED PREDOMINANTLY WITH LITHIUM

The previous section described the basic effects of adding lithium as an impurity to n- and p-type, oxygen-containing silicon which already had in it the primary doping impurity. In p-type silicon, lithium had no effect on either the observable damage centers (chiefly the K-center) or the properties of n/p solar cells. In n-type silicon, interaction between lithium and A-centers was strongly indicated; yet the presence of lithium had little, if any, effect on the radiation resistance of p/n solar cells (before annealing).

In an effort to promote the interaction of lithium with radiation-induced defects, studies were begun on silicon which had very low oxygen concentrations and which contained lithium as the dominant n-type dopant. These two experimental conditions might be expected to foster the interaction of lithium with radiation-induced defects on two accounts: (1) Since, in oxygen-containing material, the shallow donor is really a (Li-O) complex, the absence of oxygen might make the isolated lithium\* more mobile and susceptible to "trapping" by other imperfections and defects. (2) The absence of phosphorus and oxygen removes the possibility of forming A-centers and E-centers, thus increasing further the likelihood of lithium interacting with whatever other defects may be formed.

Accordingly, n-type silicon with quoted oxygen concentrations<sup>1,2</sup>  $\approx 2 \times 10^{15}/\text{cm}^3$  and resistivity  $\approx 12 \Omega\text{-cm}$  (due to  $4 \times 10^{14}/\text{cm}^3$  phosphorus) was diffused with lithium from a Li-Sn alloy at

---

\* While (Li-O) acts as a shallow donor with an energy level about 0.039 eV below the conduction band, isolated lithium is reported to be a shallow donor with an energy level about 0.033 eV below the conduction band. (T. E. Gilmer, et al., J. Phys. Chem. Solids. **26**, 1195 (1965)).

400°C to a resistivity of 0.3 to 0.4  $\Omega$ -cm and a lithium concentration of about  $2 \times 10^{16}/\text{cm}^3$ . This material was bombarded by a 1-MeV electron flux of  $1 \times 10^{16}/\text{cm}^2$  at room temperature. EPR properties of the samples were then measured at 27°K using a Varian heterodyne spectrometer operating at 9.1 GHz.\*

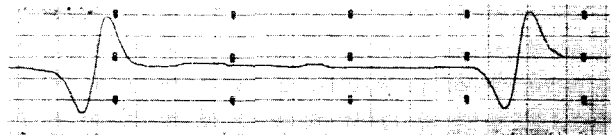
Figure 6 contains the significant EPR results of our first experiments. (In all our spectra, the spin densities have been calculated from the EPR lines of conduction electrons and of the phosphorus donor electrons in samples where these electron concentrations have been independently measured.) The first spectrum is that of a standard "calibrating" sample of silicon showing the phosphorus doublet line corresponding to a spin density (known phosphorus doping) of  $2 \times 10^{16}/\text{cm}^3$ . The doublet has a separation of about 39 gauss and is symmetrically located about a point very close to the "free" conduction electron line. (All spectra to be shown are aligned so that their magnetic field values  $H$  are the same.) The second spectrum is that of "low-oxygen" silicon and shows only the phosphorus doublet for which a spin density of  $6 \times 10^{14}/\text{cm}^3$  is calculated from spectrum 1, and is to be compared with the phosphorus concentration of  $4 \times 10^{14}/\text{cm}^3$ , the value obtained from its resistivity. The very small signal between the phosphorus lines is most likely due to some very small concentration of contaminants, surface states, etc. The third spectrum is of lithium-diffused material. A single line is observed with a spin density of  $1.3 \times 10^{15}/\text{cm}^3$ . It has no discernible angular dependence. Since its spin density is about the same as the oxygen concentration, and since an EPR absorption is not seen in oxygen-free silicon, the resonance line is almost certainly due to the (Li-O) donor. This, of course, is apart from the fact that resistivity measurements indicate that we have  $2 \times 10^{16}/\text{cm}^3$  unassociated lithium atoms which are acting as shallow donors. The fourth spectrum is of material which has not had any impurity added to it, but has been bombarded by a 1-MeV electron flux of  $1 \times 10^{16}/\text{cm}^2$ . No EPR absorption is detected and, in fact, the phosphorus doublet has disappeared. The fifth spectrum is that of lithium-doped silicon which has been electron-irradiated. Now a new resonance absorption appears about five times larger than that due to lithium alone, spectrum three (note different gains for different parts of this spectrum). In addition, the phosphorus doublet lines are now present, in contradistinction to the case of spectrum four. Again, no measurable angular dependence of the new center is observed. It is to be stressed that (1) this new larger resonance line appears *only* in material which both contains lithium and has been electron-irradiated and (2) the phosphorus doublet is caused to disappear by either lithium alone or electron-irradiation alone, but *not* by the combination of the two.

In Fig. 7 are shown the effects of the presence of high oxygen concentrations and of bombardment flux levels on the lithium paramagnetic resonance. The first spectrum is again the calibrated phosphorus doublet line. The second spectrum is that of "low-oxygen" silicon containing lithium alone. The third is that of lithium alone in silicon containing about  $10^{18}/\text{cm}^3$  oxygen. Note that although the resistivities of both silicon samples are the same, i.e., the lithium donor concentrations are the same ( $\approx 2 \times 10^{16}/\text{cm}^3$ ), EPR absorption of the sample

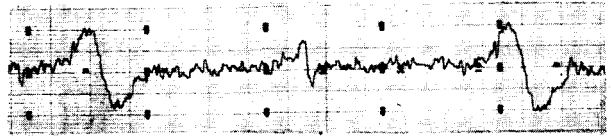
---

\* Further details of the EPR equipment may be found in the Semiannual Report dated July 7, 1965.

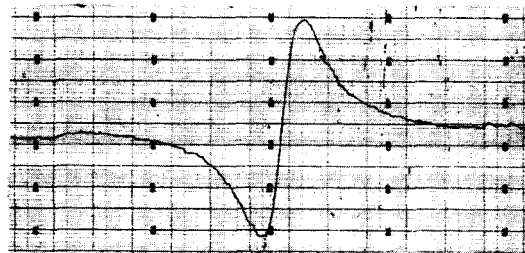
PHOSPHORUS DOUBLET:  
 $N_D = 2 \times 10^{16}/\text{cm}^3$   
 SPIN DENSITY =  $1.8 \times 10^{16}/\text{cm}^3$   
 GAIN = 40



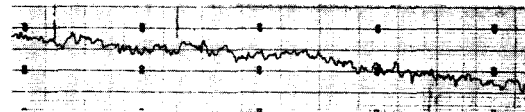
OXYGEN CONCENTRATION =  $1.2 \times 10^{15}/\text{cm}^3$   
 PHOSPHORUS  $N_D = 4 \times 10^{14}/\text{cm}^3$   
 SPIN DENSITY =  $6 \times 10^{14}/\text{cm}^3$   
 LITHIUM = 0  
 $\phi = 0$   
 GAIN = 800



OXYGEN CONCENTRATION =  $1.2 \times 10^{15}/\text{cm}^3$   
 LITHIUM  $N_D = 2 \times 10^{16}/\text{cm}^3$   
 SPIN DENSITY =  $1.3 \times 10^{15}/\text{cm}^3$   
 PHOSPHORUS  $N_D = 4 \times 10^{14}/\text{cm}^3$   
 SPIN DENSITY = 0  
 $\phi = 0$   
 GAIN = 250



OXYGEN CONCENTRATION =  $1.2 \times 10^{15}/\text{cm}^3$   
 PHOSPHORUS  $N_D = 4 \times 10^{14}/\text{cm}^3$   
 SPIN DENSITY = 0  
 LITHIUM = 0  
 $\phi = 1 \times 10^{16}/\text{cm}^2$   
 GAIN = 800



OXYGEN CONCENTRATION =  $1.2 \times 10^{15}/\text{cm}^3$   
 LITHIUM  $N_D = 2 \times 10^{16}/\text{cm}^3$   
 SPIN DENSITY =  $6 \times 10^{15}/\text{cm}^3$   
 PHOSPHORUS  $N_D = 4 \times 10^{14}/\text{cm}^3$   
 SPIN DENSITY =  $5 \times 10^{14}/\text{cm}^3$   
 $\phi = 1 \times 10^{16}/\text{cm}^2$   
 GAIN = 500-200-500

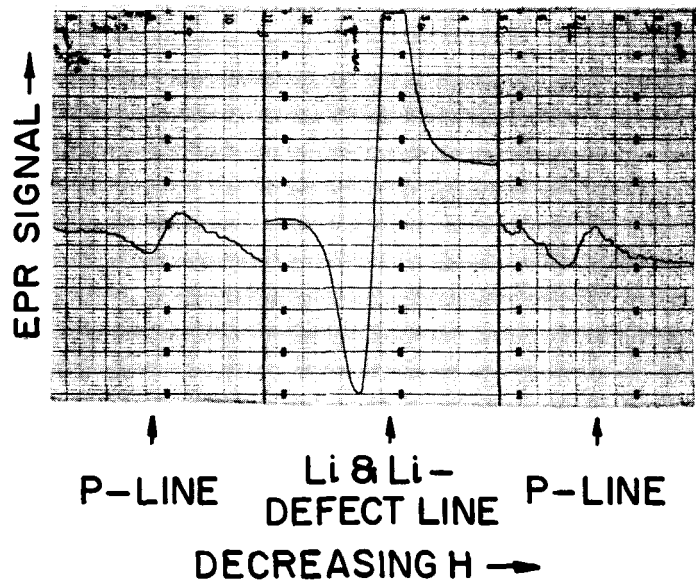


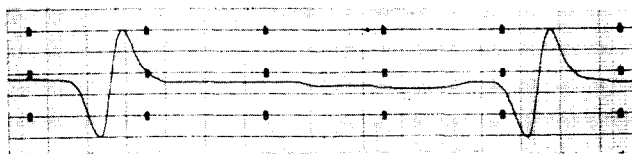
Fig. 6. Significant EPR results.

PHOSPHORUS DOUBLET

$$N_D = 2 \times 10^{16}/\text{cm}^3$$

$$\text{SPIN DENSITY} = 1.8 \times 10^{16}/\text{cm}^3$$

$$\text{GAIN} = 40$$



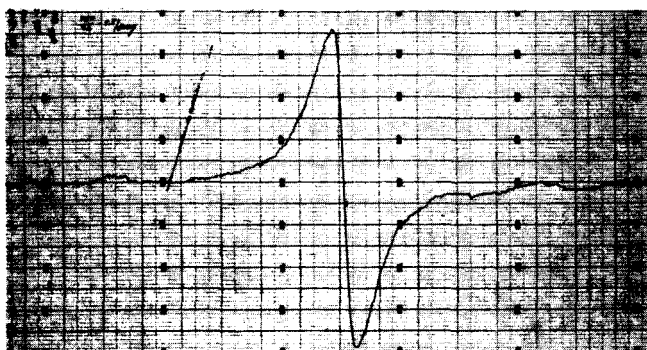
$$\text{OXYGEN CONCENTRATION} = 1.2 \times 10^{15}/\text{cm}^3$$

$$\text{LITHIUM } N_D = 2 \times 10^{16}/\text{cm}^3$$

$$\text{SPIN DENSITY} = 1.8 \times 10^{15}/\text{cm}^3$$

$$\phi = 0$$

$$\text{GAIN} = 400$$



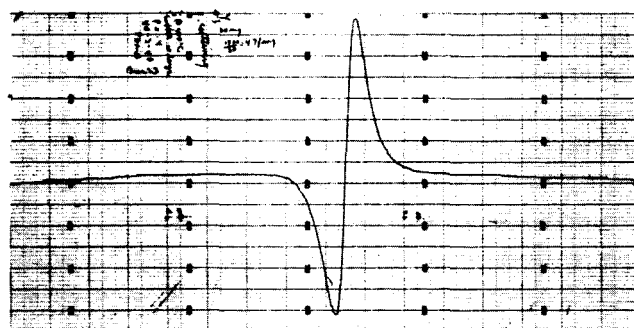
$$\text{OXYGEN CONCENTRATION} = 10^{18}/\text{cm}^3$$

$$\text{LITHIUM } N_D = 2 \times 10^{16}/\text{cm}^3$$

$$\text{SPIN DENSITY} = 1.5 \times 10^{16}/\text{cm}^3$$

$$\phi = 0$$

$$\text{GAIN} = 40$$



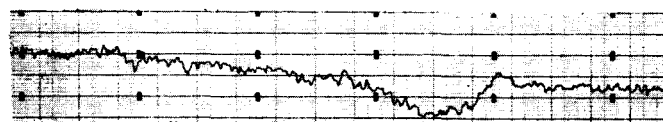
$$\text{OXYGEN CONCENTRATION} = 1.2 \times 10^{15}/\text{cm}^3$$

$$\text{LITHIUM } N_D = 2 \times 10^{16}/\text{cm}^3$$

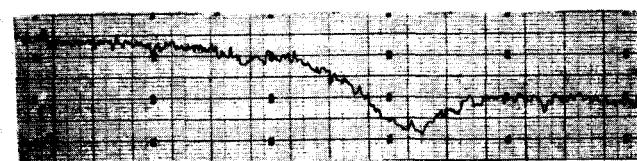
$$\text{SPIN DENSITY} = 0$$

$$\phi = 3 \times 10^{16}/\text{cm}^2$$

$$\text{GAIN} = 800$$



$$\text{SAME AS ABOVE EXCEPT } \phi = 5 \times 10^{16}/\text{cm}^2$$



EPR SIGNAL

↑                      ↑                      ↑                      ↑  
 P-LINE    Li-LINE    DAMAGE    P-LINE  
 DECREASING H →

Fig. 7. Effects of high oxygen concentration and of bombardment flux level on the Li paramagnetic resonance.

containing  $\approx 10^{18}/\text{cm}^3$  oxygen is about 10 times that of the sample which contains  $\approx 2 \times 10^{15}/\text{cm}^3$  oxygen. The fourth and fifth spectra are of "low-oxygen" silicon containing lithium, bombarded with electron fluxes of  $3 \times 10^{16}/\text{cm}^2$  and  $5 \times 10^{16}/\text{cm}^2$ , respectively. The lithium line has completely disappeared, either because the deep damage centers\* have captured the shallow donor electrons, or because the Fermi level has moved sufficiently deep into the forbidden energy region to ionize all the Li or (Li-O) donor levels. The appearance of the damage center spectra are somewhat reminiscent of those produced by high electron fluxes and shown in the previously issued Semiannual Report\*\* in Fig. 15.

The important practical effects of the new Li-defect center (hereafter called the L-center) seen in Fig. 6, curve 4, would be the effects it has on solar cell properties and the rate at which these effects occur. In Section III these are discussed in terms of electrical properties and solar cell parameters.<sup>†</sup> Here, we have made preliminary measurements of time effects as measured by EPR techniques. Figure 8 shows first the phosphorus doublet lines, then the resonance line due to lithium alone, and finally the new L-center line taken after 1, 4¼, 25 hours, and 1 month at room temperature after the electron irradiation. Note that the new center's resonance has decreased markedly during this time, indicating a spontaneous annealing of this damage center. No other new center is seen during this room-temperature annealing.

### C. DISCUSSION

The EPR measurements described in Section B. have unambiguously illustrated several very important features of electron-irradiated, lithium-doped, "low-oxygen" silicon. Perhaps the most important is that a new center, the L-center, is formed which must involve lithium and the radiation-produced damage center.

This center is different in character from previously reported damage centers. Its EPR spectrum consists of but one line with no measurable angular dependence in contradistinction to the very strong angular dependence of several resonance lines generally observed for the deeper ( $\gtrsim 0.2$  eV) damage centers.

Neither oxygen nor phosphorus appear to be part of this center, since its concentrations are about 5 times the oxygen concentration, and when the L-center appears, the phosphorus doublet (representing as it does the isolated phosphorus atom) is simultaneously observed. Note that while lithium alone or electron-irradiation alone cause the phosphorus doublets to disappear, the combination of two (i.e., the L-center) does not.

The stability of the L-center appears to be quite low. Figure 8 illustrates that the L-center anneals out spontaneously at room temperature, although an appreciable level, about 35%, still remains after a month. This suggests (but does not absolutely indicate) that the L-center's

---

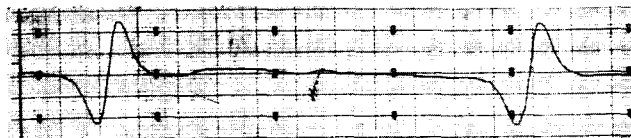
\* Most likely C-centers or lithium-C-center complexes.

\*\* B. Goldstein et al., Semiannual Report, Contract No. NAS5-9131, July 1965.

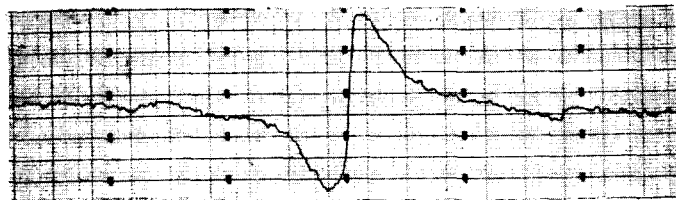
† One should always bear in mind, however, that a defect seen by a measurement such as EPR may not be the defect primarily responsible for the degradation of lifetime or other solar cell properties.



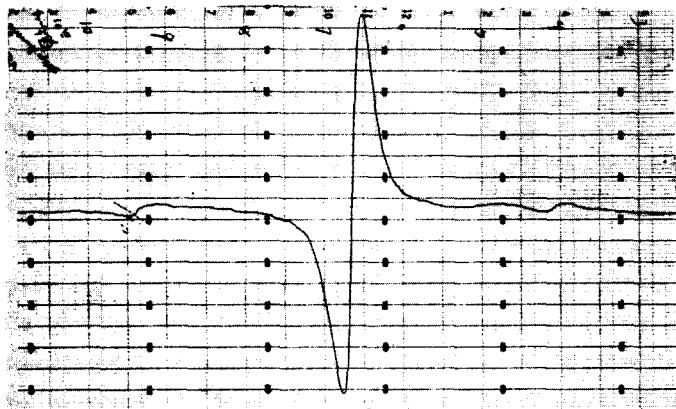
PHOSPHORUS DOUBLET  
 $N_D = 2 \times 10^{16}/\text{cm}^3$   
 SPIN DENSITY =  $1.8 \times 10^{16}/\text{cm}^3$   
 GAIN = 40



OXYGEN CONCENTRATION =  $1.2 \times 10^{15}/\text{cm}^3$   
 LITHIUM  $N_D = 2 \times 10^{16}/\text{cm}^3$   
 SPIN DENSITY =  $1.8 \times 10^{15}/\text{cm}^3$   
 PHOSPHORUS  $N_D = 4 \times 10^{14}/\text{cm}^3$   
 SPIN DENSITY = 0  
 $\phi = 0$   
 GAIN = 400

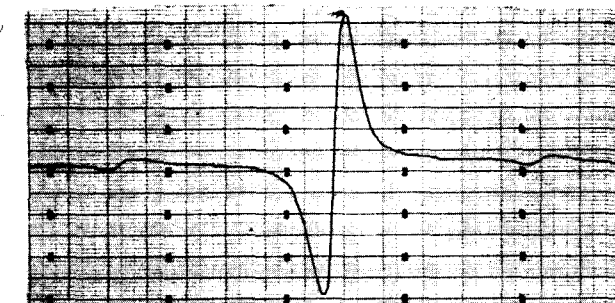


OXYGEN CONCENTRATION =  $1.2 \times 10^{15}/\text{cm}^3$   
 LITHIUM  $N_D = 2 \times 10^{16}/\text{cm}^3$   
 PHOSPHORUS  $N_D = 4 \times 10^{14}/\text{cm}^3$   
 $\phi = 5 \times 10^{15}/\text{cm}^2$   
 $t = 1 \text{ hr.}$   
 SPIN DENSITY =  $9.0 \times 10^{15}/\text{cm}^3$   
 GAIN = 100

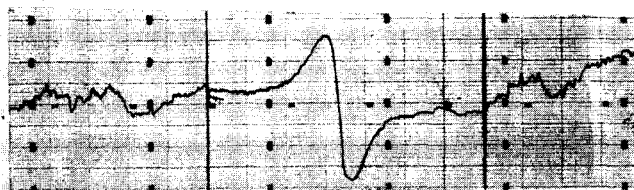


$t = 4.25 \text{ hr.}$   
 SPIN DENSITY =  $6.5 \times 10^{15}/\text{cm}^3$   
 GAIN = 100

EPR SIGNAL ↑



$t = 720 \text{ hr.}$   
 SPIN DENSITY =  $3.5 \times 10^{15}/\text{cm}^3$   
 GAIN = 800-100-800



↑                      ↑                      ↑  
 P-LINE              Li & Li              P-LINE  
                          DEFECT LINE  
 DECREASING H →

Fig. 8. EPR data for the phosphorus doublet lines, the resonance line due to lithium alone, and the new L-center line at different times.

binding energy is quite low. This is further indicated by the fact that a 10-minute 80°C heat treatment produced about a 50% diminution of the L-center. One experimental fact does suggest strongly that the L-center dissociates; i.e., as the L-center decreases with time, as shown in Fig. 8, the phosphorus doublet also decreases. We had seen in Fig. 6 that lithium alone or the radiation-produced defect alone caused the phosphorus doublet to disappear. Finally, it should be noted that the time constant of the L-center's annealing is of the order of a day. As we shall see, this does not relate in any simple way to the time constant of the recovery of solar cell damage.

The model for the L-center and the mechanism of its formation can only be speculated on at this time, but there are some considerations which are applicable. It is likely that a 1-MeV electron basically produces (chiefly) vacancies and a much smaller number of divacancies. This is based on known introduction rates. The vacancy has been shown to be a surprisingly mobile defect at room temperature. So, of course, is lithium. The introduction rate for the L-center is about 0.5/cm. Thus, a first speculation is that the L-center is a Li-vacancy complex. Its energy level should be shallow, of the same order of the phosphorus energy level, because if its level were appreciably deeper, the resulting Fermi level would likely cause the phosphorus to lose its donor electron and thus its EPR absorption.

If the most likely model for the L-center is a Li-vacancy complex, based on the high introduction rate and the high mobility of the constituent elements, the mechanism of its formation is obscure at this time. The fact that the L-center appears to be independent of oxygen and phosphorus does not mean that these elements play no role in the L-center's formation. It is possible that the A-center or E-center may be an intermediate and/or transient step in the L-center's formation.

The significance of the formation mechanism will become more apparent in the next section on electrical and solar cell measurements. A summary discussion of EPR and solar cell results is given in Section IV.

### III. INCREASED RADIATION RESISTANCE OF SOLAR CELLS THROUGH THE USE OF LITHIUM

#### A. INTRODUCTION

A major goal of this study has been to find an impurity which would interact with radiation-induced defects in silicon to form centers which preserve the minority-carrier diffusion length,  $L$ . Such an impurity would lead to more radiation-resistant solar cells and other devices. A number of potentially useful impurities were investigated; among these were Li, Cu, Al, Gd and Fe; the results of the latter four were described in detail in earlier reports. Lithium alone proved to merit further study. The culmination of this study, as will be seen below, was the fabrication of solar cells with remarkably increased radiation-resistant properties.

#### B. EXPERIMENTAL DETAILS OF THE LITHIUM STUDY

Throughout this study, the basic device parameter which was examined was  $L$ , measured by the electron-voltaic effect,<sup>10</sup> as a function of flux. Initially,  $L$  was measured in surface barriers on n-type and lithium-diffused n/p junctions in p-type silicon. Although the potential usefulness of lithium could be seen with these structures, they had disadvantages which indicated that well-defined junctions uniformly doped with lithium were necessary in continuing this study. The disadvantage of the lithium-diffused n/p junctions, for example, was the experimental difficulty of separating increases in base resistivity due to lithium, from lithium-damage-center interactions in the observed radiation resistance. The photovoltaic properties of the surface barriers, on the other hand, were obscured by the interfering gold contact on the top surface. Hence, measurements other than the electron-voltaic effect were not easily interpreted.

While not suitable for continued study, the early structures did delineate the procedures to be followed in making lithium effective in solar cells. For example, the surface-barrier results clearly showed the importance of the relative concentrations of lithium, oxygen, and phosphorus on the radiation behavior of the device. This information was vital to the solar-cell work which followed.

Another observation from the early work was the need to consider the lithium distribution in the device in interpreting the results of the damage experiments. It was found, for example, that  $L$  in lithium-doped surface barriers matched closely the value in undoped samples in spite of an apparent difference in material resistivity. Four-point-probe measurements typically showed the resistivity of the lithium-doped samples to be lower than in the undoped samples by at least an order of magnitude. Subsequent examination of the lithium distribution itself, by capacitance and resistivity measurements, however, indicated that the base resistivity near the barrier in both lithium-doped and undoped specimens was closer in value than the four-point-probe measurements indicated. This explained why  $L$  in both specimens was the same. It was also found that from resistivity profiles of the first n/p solar cells "uniformly" doped with lithium that the distribution could be so nonuniform that regions of n-type conductivity were included in the p-type region. (EPR measurements of some samples gave similar results.) Such nonuniformity could be expected to have a harmful effect on the electrical properties of these cells.

With the above considerations in mind, a procedure was evolved for making lithium-doped solar cells. This procedure generally consisted of the following steps for p/n cells; n/p cells were made in a similar fashion with appropriate change in impurity where required. Boron was diffused into high-resistivity ( $\rho > 10 \Omega\text{-cm}$ ), floating-zone, n-type silicon to form a p/n junction. Lithium was then diffused into the material from a suitable source, such as a lithium-oil paste or a lithium-tin alloy, at approximately  $400^\circ\text{C}$  for times up to 24 hours. The lithium concentration was estimated from resistivity measurements. The cell was completed by evaporating Ag:Ti contacts and a SiO antireflection coating on the appropriate side of the junction. (Contact sintering was tried with no apparent effect on the final results.) Capacitance measurements were made on the completed device to obtain the lithium concentration in the junction region.

The photovoltaic and electron-voltaic properties of these cells were studied and are reported below. The damaging particles used were mainly 1-MeV electrons. However, data will also be presented from a 16.8-MeV proton and a low-level gamma experiment.

### C. n/p SOLAR CELLS

Floating-zone (F.Z.) and quartz-crucible (Q.C.) n/p cells containing lithium were irradiated, but no clear interaction of lithium with radiation defects was observed in the electrical measurements.

Before the addition of lithium, the base resistivities  $\rho$  in the cells ranged from 2.5 to  $14 \Omega\text{-cm}$ . The cells were immersed in a lithium-tin bath for a time sufficiently long to establish a reasonably uniform lithium concentration. The added lithium concentration was approximately  $2 \times 10^{15} \text{ cm}^{-3}$  in the lower- $\rho$  cells and  $5 \times 10^{14} \text{ cm}^{-3}$  in the higher- $\rho$  cells.

Typical behavior observed in one group of F.Z. cells is shown in Fig. 9. The value of  $L$  is seen not to depend upon the presence of lithium. Furthermore, no recovery of  $L$  was observed after irradiation. The four-point resistivities on the backside and those deduced from capacitance measurements,  $\rho_c$ , are shown in Fig. 9. These values indicate that lithium was indeed in the junction region and was reasonably uniform in the base region.

These results are in agreement with the picture which is emerging in this study. This picture supposes that lithium must compete with the other impurities in the material for the radiation-induced vacancies (or other damage centers) to form a different damage-center complex. On this basis, then, the lithium concentration must exceed the concentrations of the other impurities, assuming comparable cross sections for the vacancy interaction. The two centers ordinarily found in p-type silicon are the J- and the K-centers. The J-center is the divacancy, an intrinsic defect which does not depend upon the impurity concentrations. The K-center, on the other hand, is known to involve oxygen and no other impurity.<sup>7</sup> Therefore, the lithium concentration must exceed the oxygen concentration before any effect can be seen. This criterion rules out Q.C. n/p cells since lithium concentrations of  $10^{17}$  to  $10^{18}/\text{cm}^3$  would be required, and the donor nature of lithium at these concentrations would convert the material to n-type, unless it was very heavily doped initially with acceptors.

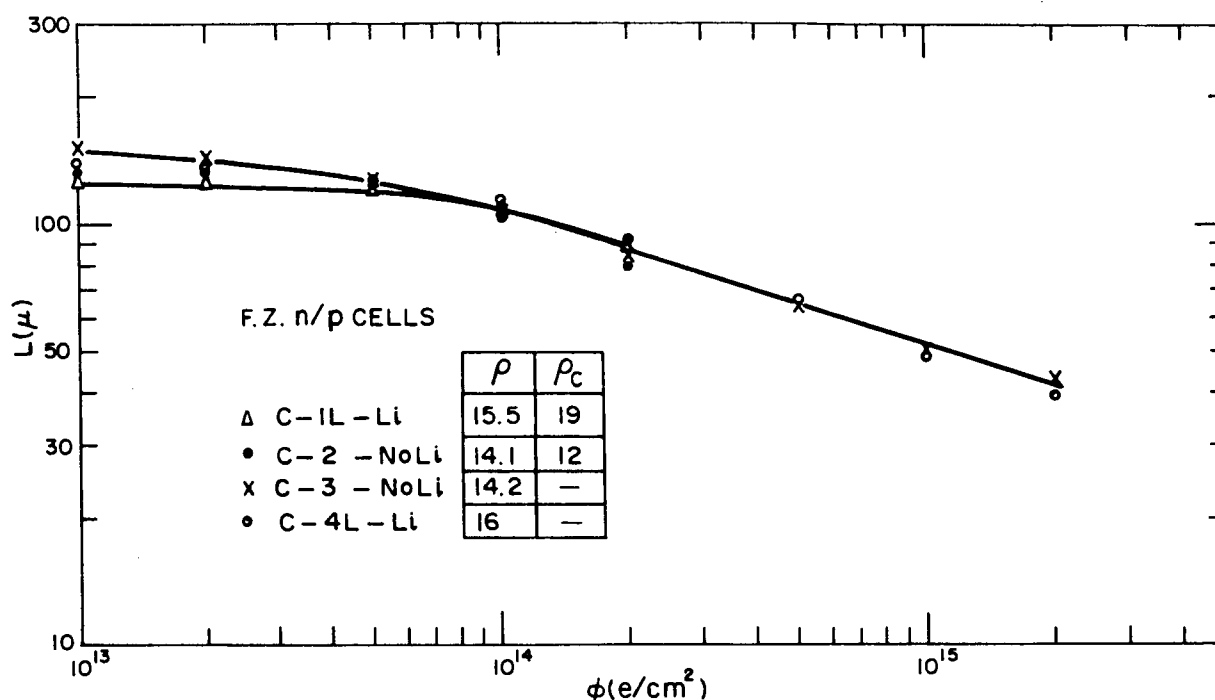


Fig. 9. Typical  $L$  vs.  $\phi$  characteristics of n/p floating-zone cells.

Another factor which tends to rule out all n/p cells, both Q.C. and F.Z., is the known pairing of lithium with acceptors<sup>11</sup> and oxygen<sup>12</sup> to form complexes which are stable at room temperature. This pairing immobilizes a large fraction of the available lithium which then is not free to react with radiation-induced defects. (Incidentally, this pairing also "neutralizes" the oxygen and reduces its reaction with defects. See Section D below for evidence of this behavior.)

Because of the negative experimental results and the above considerations concerning the difficulty of achieving the proper lithium, oxygen and acceptor concentrations, no further work is contemplated on the n/p cell at this time.

## D. p/n SOLAR CELLS

### 1. Electron Irradiations

The difficulties of obtaining the proper lithium concentrations mentioned above do not exist in p/n structures because lithium itself can supply the donor electrons required for the n-type conductivity. It was found in fact, that when the lithium concentration exceeds both the oxygen and other donor concentrations in the n-type region, the resultant cells are currently the most radiation-resistant ones available. As pointed out above, this discovery stemmed essentially from the early surface-barrier studies, whose results can be summarized as follows:

1. Lithium diffused into 10- $\Omega$ -cm F.Z. material to a level of  $\approx 10^{16}/\text{cm}^3$  resulted in surface barriers which showed large room-temperature recovery of L after irradiation.
2. Lithium diffused into 1- $\Omega$ -cm (phosphorus-doped) F.Z. material to a level of  $\approx 10^{16}/\text{cm}^3$  did not lead to improved radiation resistance.
3. Lithium diffused into Q.C. material to a level of  $\approx 10^{16}/\text{cm}^3$  did not lead to an improvement in radiation resistance.
4. The heat treatment associated with the lithium diffusion, by itself, did not lead to radiation-resistant devices (this was a "control" experiment).

Thus, the criterion was established that the lithium concentration must exceed both the oxygen and other donor concentrations before an effect could be seen. In other words, lithium must be the dominant impurity in the n-type region. This result is understandable in the framework of a competition of lithium with the other impurities for the radiation-induced vacancies. When, for example, the oxygen concentration exceeds the other impurity concentrations, the vacancy-oxygen or A-center will form preferentially to any other center. Similarly, when phosphorus is the dominant impurity, the vacancy-phosphorus, or E-center, will be formed. One expects then, as indeed our results show, that, when the lithium concentration is the dominant one, a new center may be formed. Direct evidence for the formation of such a new center is reported and discussed in the EPR studies of Section II. Fortunately, the recombination properties of the new center are much less damaging than those of the A- or E-centers.

Further corroboration of these ideas, as well as evidence for the pairing of lithium and oxygen\*, were obtained in an experiment with cells which were purchased as F.Z. cells, but which had more oxygen (actually  $\lesssim 3 \times 10^{17}/\text{cm}^3$ ) than originally supposed. The phosphorus and added lithium concentration in these cells was  $\approx 7 \times 10^{15}/\text{cm}^3$  and  $\approx 10^{16}/\text{cm}^3$ , respectively. Upon irradiation, the data shown in Fig. 10 were obtained. The value of L in the lithium-diffused cells behaved quite alike that in the untreated cells; none of the cells showed any substantial recovery after irradiation. Subsequent isochronal annealing measurements on similar cells revealed, however, the surprising behavior shown in Fig. 11. The fraction of damage f remaining in the short-circuit current measured in filtered incandescent light is shown for two cells cut from the same parent crystal and irradiated together to a flux of  $1 \times 10^{14} \text{ e}/\text{cm}^2$ . The cell diffused with lithium has an annealing behavior much different from that of the untreated cell. The lithium cell shows a primary annealing stage at  $\approx 100^\circ\text{C}$  and a secondary stage at  $\approx 225^\circ\text{C}$ . Only reverse-annealing at  $\approx 225^\circ\text{C}$  is seen in the untreated cell. It is easy to understand this behavior if the annealing stage at  $100^\circ\text{C}$  is associated with the E-center, and the remaining stage (and the reverse-annealing in the untreated cell at  $\approx 225^\circ\text{C}$ ) with the A-center. Then, the argument is that lithium paired with the oxygen in the material to reduce the A-center formation, and to enhance the remaining interaction, namely, the E-center formation. The apparent difficulty here was that the (F.Z.) material should have contained little ( $\lesssim 10^{16}/\text{cm}^3$ ) oxygen. To resolve this difficulty, the oxygen content was checked by a 9- $\mu$  optical measurement,<sup>13</sup> as well as by a heat treatment<sup>14</sup>

---

\* For other direct evidence, see the EPR results of Fig. 6.

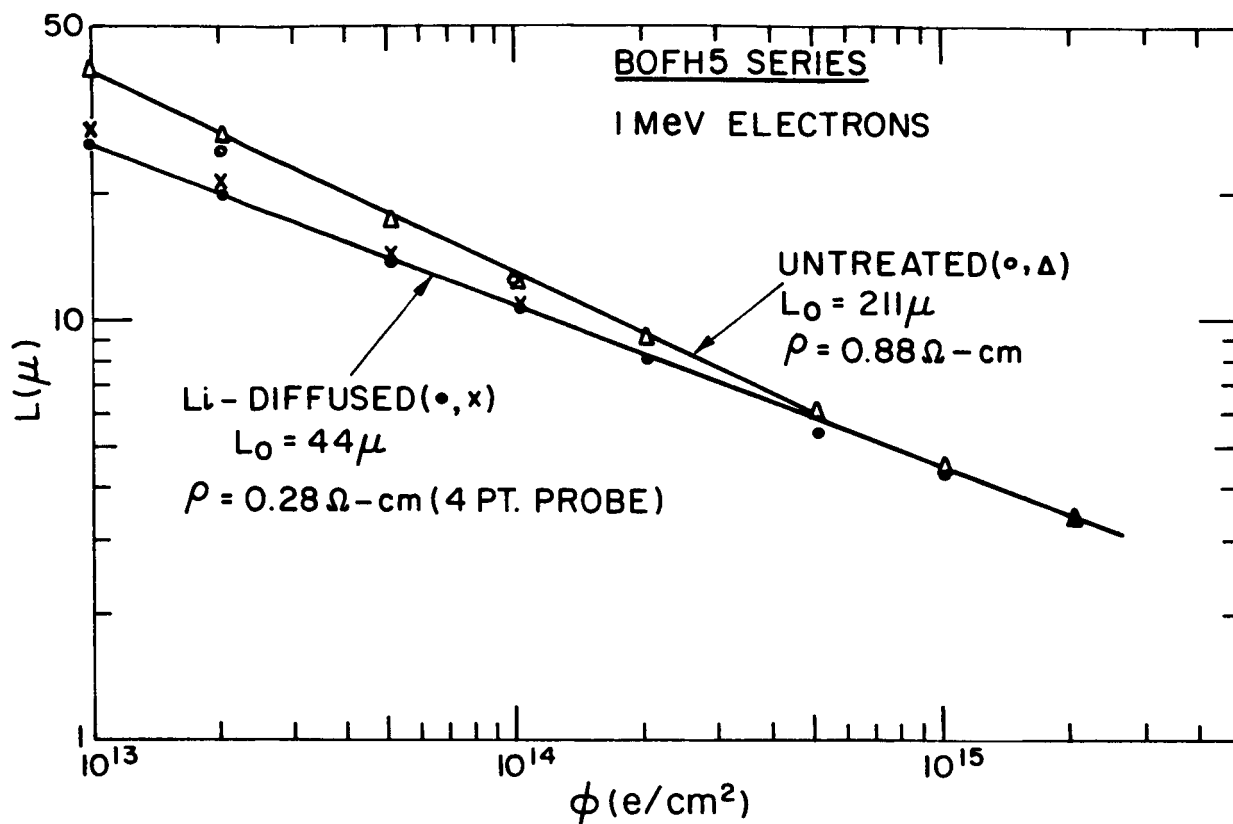


Fig. 10. Result of irradiation of Li-diffused F.Z. cells.

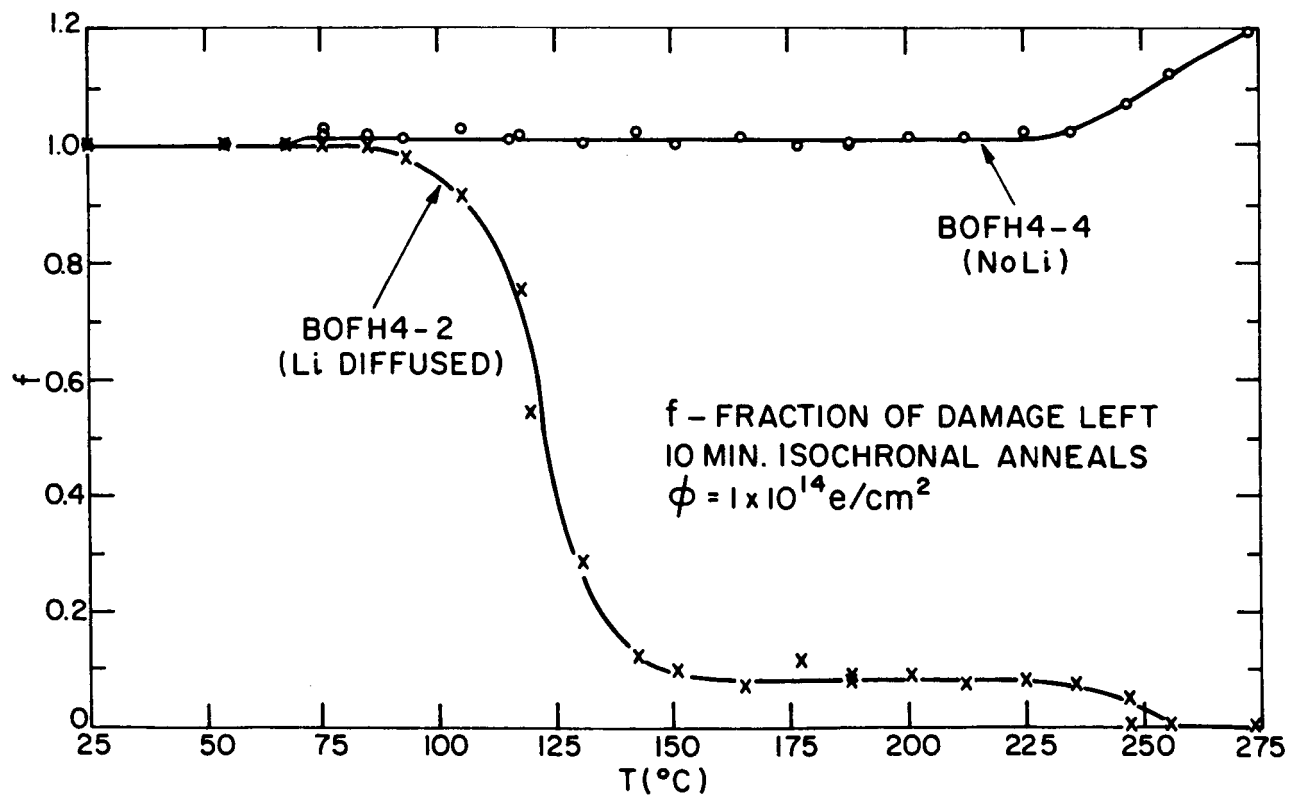


Fig. 11. Annealing behavior of Li-diffused F.Z. cells.

which would form donors if oxygen were present. Both measurements established that the material did indeed contain oxygen. Only an upper limit to this concentration could be obtained, however, because of free-carrier absorption and the consequent difficulty in determining the absorption due solely to oxygen. This upper limit was  $3 \times 10^{17}/\text{cm}^3$ . This experiment, then, added support to the ideas evolving in this study.

Logically, the investigation turned next to F.Z. p/n cells in which lithium was the dominant impurity in the base region. It was established that the oxygen content of the material was  $\ll 10^{17}/\text{cm}^3$  and the phosphorus content was  $\approx 2 \times 10^{14}/\text{cm}^3$ . The lithium concentration near the junction was determined from capacitance measurements and compared with the four-point-probe resistivity measurement on the backside of the cell. These measurements indicated the lithium distribution was not uniform, resulting in a drift-field which in itself should enhance the radiation-resistance of these cells. However, the magnitude of this field was computed to be only of the order of 1 V/cm; this field is thus too small to affect the results. This conclusion was verified on other cells fabricated with a more uniform lithium distribution. The results with these cells were similar to those obtained with the cells having the more nonuniform distribution.

The behavior of  $L$  vs.  $\phi$  in a lithium-doped cell and in a standard cell is shown in Fig. 12. The standard cell is defined as a F.Z. cell from the group out of which the lithium-doped cell was made. The radiation rate was  $1 \times 10^{14} \text{ e/cm}^2/\text{hr}$  or greater. Periodically, the irradiation was stopped and the room-temperature recovery measured.

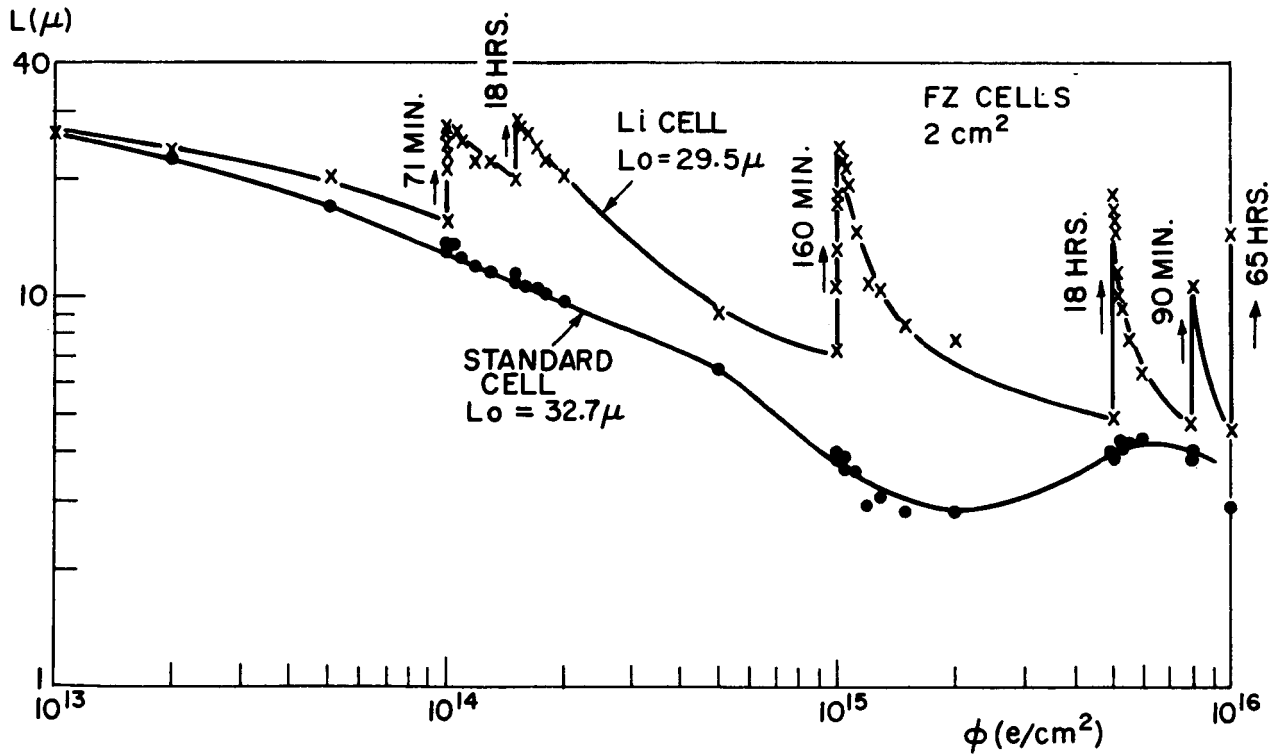


Fig. 12. Behavior of  $L$  vs.  $\phi$  in a Li-doped cell and a standard cell.



It is seen that during irradiation the damage is introduced at a comparable rate in both cells. When bombardment is stopped, however, L recovers only in the lithium cell. This recovery occurs throughout the flux range shown, whenever bombardment is stopped. The standard cell behaves anomalously around  $1 \times 10^{15} \text{ e/cm}^2$  where L drops rapidly with flux and then recovers somewhat. This behavior is attributed to movement of the Fermi level, due to carrier-removal sites introduced by bombardment. The introduction rate of these sites may be  $\approx 0.1/\text{cm}$ ; thus,  $10^{14}/\text{cm}^3$  carriers are removed in this range, a number comparable to the initial donor concentration of  $2 \times 10^{14}/\text{cm}^3$ .

The significant features of the data in Fig. 12 are that the degradation rate in both cells during bombardment is similar with this irradiation rate and that the lithium-diffused cell alone recovers after bombardment. The apparent rapid drop in L in the lithium cell upon subsequent bombardment is actually due to the manner chosen to present the data. An integrated flux scale is used for convenience to represent the bombardment. Since the recovery signifies an annealing of damage, subsequent irradiation should then be plotted on a new scale, instead of being compressed into an integrated flux scale. This compression results in an apparently more rapid degradation than does in fact exist. This is verified in Fig. 13 where the data in Fig. 12 have been replotted moving the recovered value of L backwards in flux until it intercepts the same value obtained before the bombardment was stopped. The result of these translations is a smooth curve which is close in value to the one for the standard cell.

The recovery of L at room temperature is shown in Fig. 14 for two fluxes. The recovery time is apparently flux-dependent with the longer time associated with the higher flux. These data require further study to establish the flux-dependence of the recovery time constant.

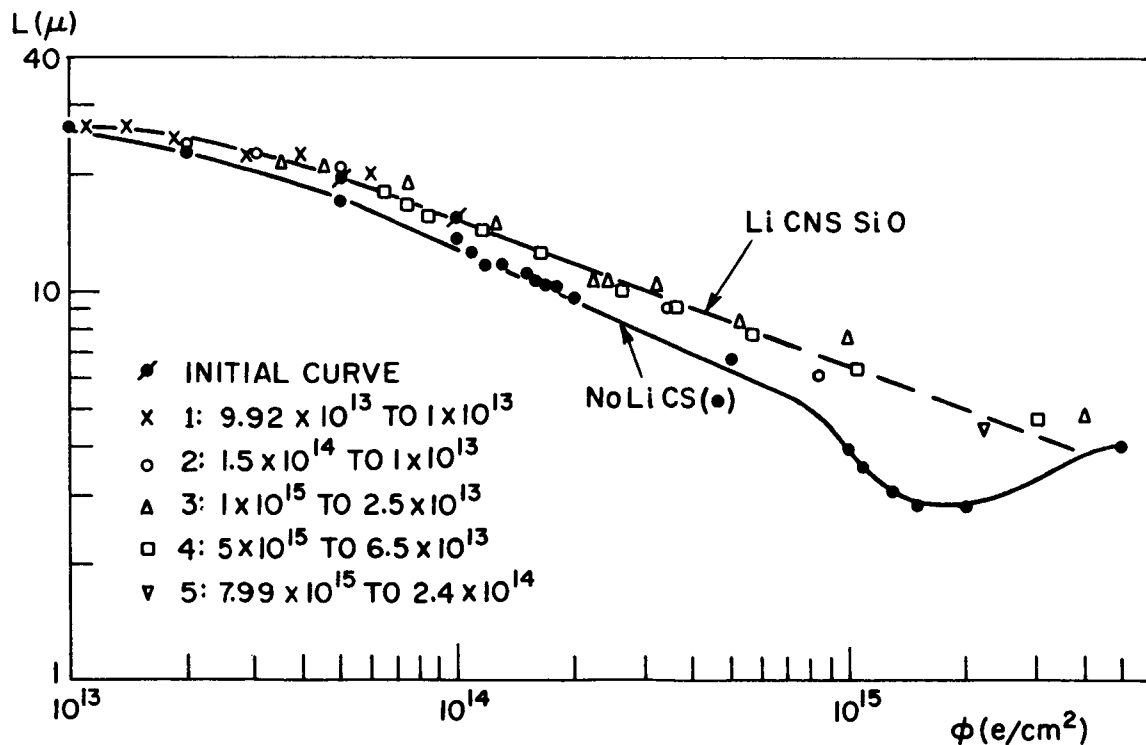


Fig. 13. Adjusted plot of L vs.  $\phi$  (Figure 12).

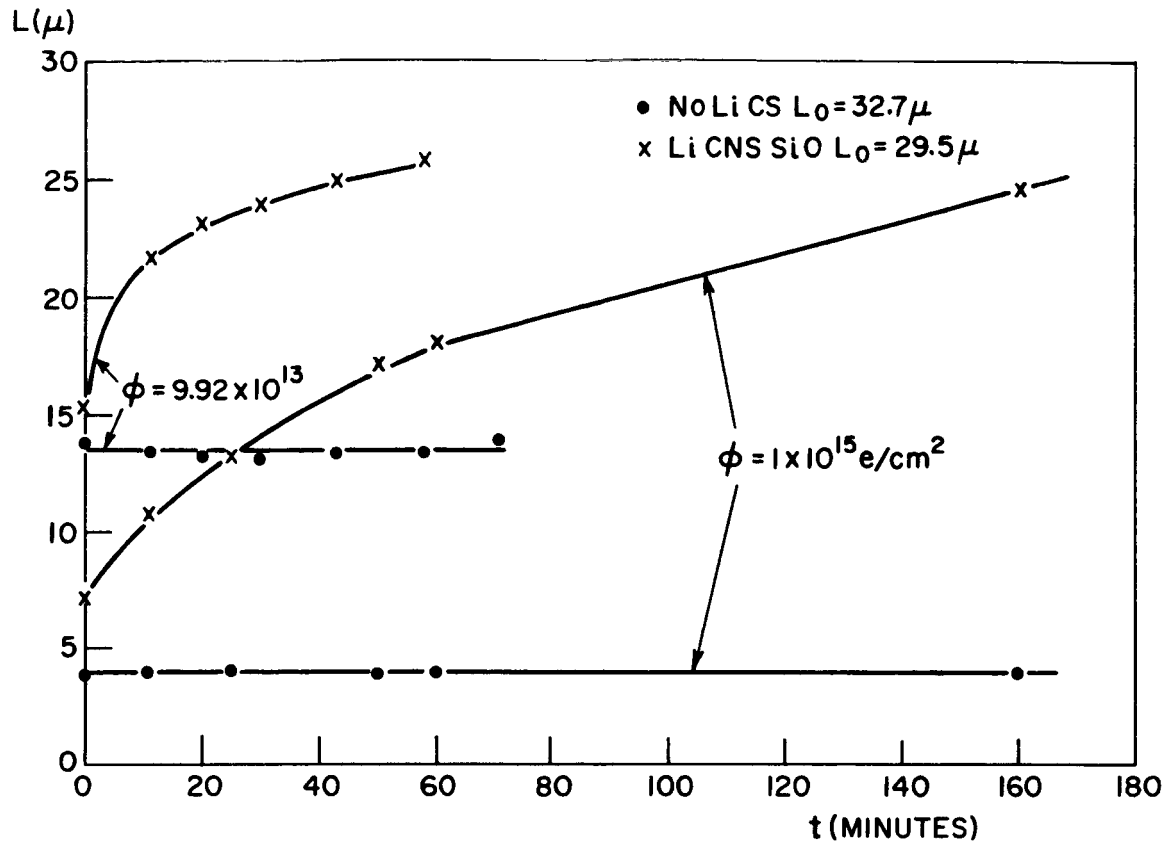


Fig. 14. Recovery of  $L$  at room temperature for two fluxes.

The effect of temperature on the recovery is shown in Fig. 15 for another lithium-doped cell. The room-temperature recovery was measured after  $1 \times 10^{14} \text{ e/cm}^2$ . The sample was then irradiated to  $2 \times 10^{14} \text{ e/cm}^2$  and placed in an ice bath at  $0^\circ\text{C}$  for 65 minutes. After this time, the sample was removed and the room-temperature recovery measured. Very little recovery occurred at  $0^\circ\text{C}$ , but when the sample warmed to room temperature, its recovery closely followed the case where the sample was not cooled after irradiation. Thus, the data after the ice bath, when translated backwards by 60 minutes, falls on the curve obtained initially at room temperature.

The data in Fig. 15 are replotted as  $(L-L_0)/(L_{AB}-L_0)$  on a semilog plot in Fig. 16. The initial diffusion length is  $L_0$ , and its value immediately after bombardment is  $L_{AB}$ . The room-temperature data initially follow an exponential relationship with time, breaking off into a second-order relationship at longer times. The time constant  $\tau$  for the initial recovery is 57 minutes. If it is assumed that the ice-bath data are also exponential,  $\tau$  at  $0^\circ\text{C}$  would be 480 minutes. The ratio  $\tau_0/\tau_{RT}$  is 8.4, a value very close to the inverse ratio of the lithium diffusion constant at these temperatures, which is 9. This result strongly suggests that the recovery process is due to the movement of lithium to (or from) the radiation defects, assuming these defects themselves do not move substantially during recovery. As discussed below, this result is important in establishing a model of the lithium interaction.

Although only the behavior of  $L$  was considered up to now, similar behavior was also seen in the photovoltaic properties of the cells. Figure 17 illustrates that the short-circuit

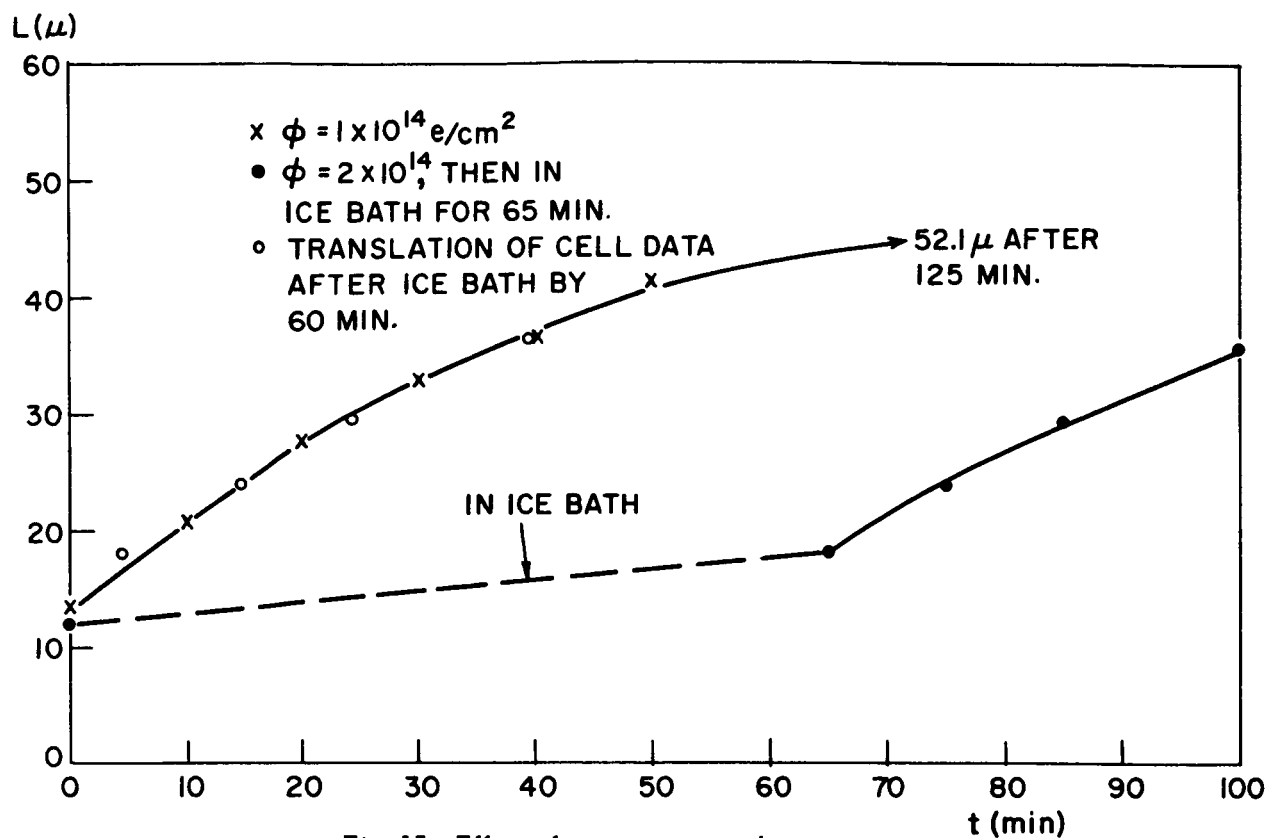


Fig. 15. Effect of temperature on the recovery.

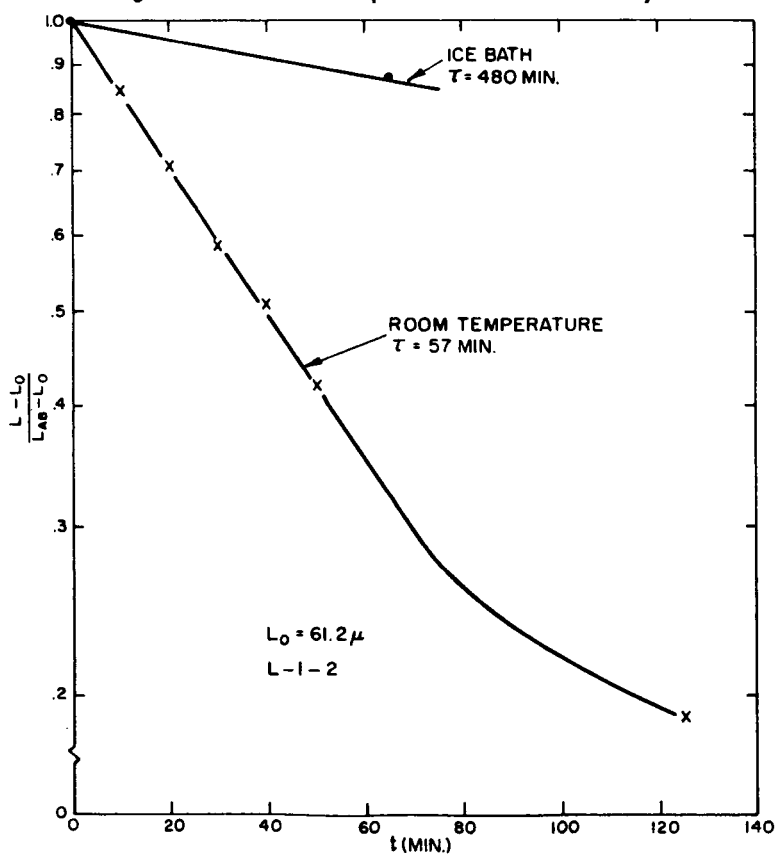


Fig. 16.  $(L-L_0)/(L_{AB}-L_0)$  plotted on semilog scale.

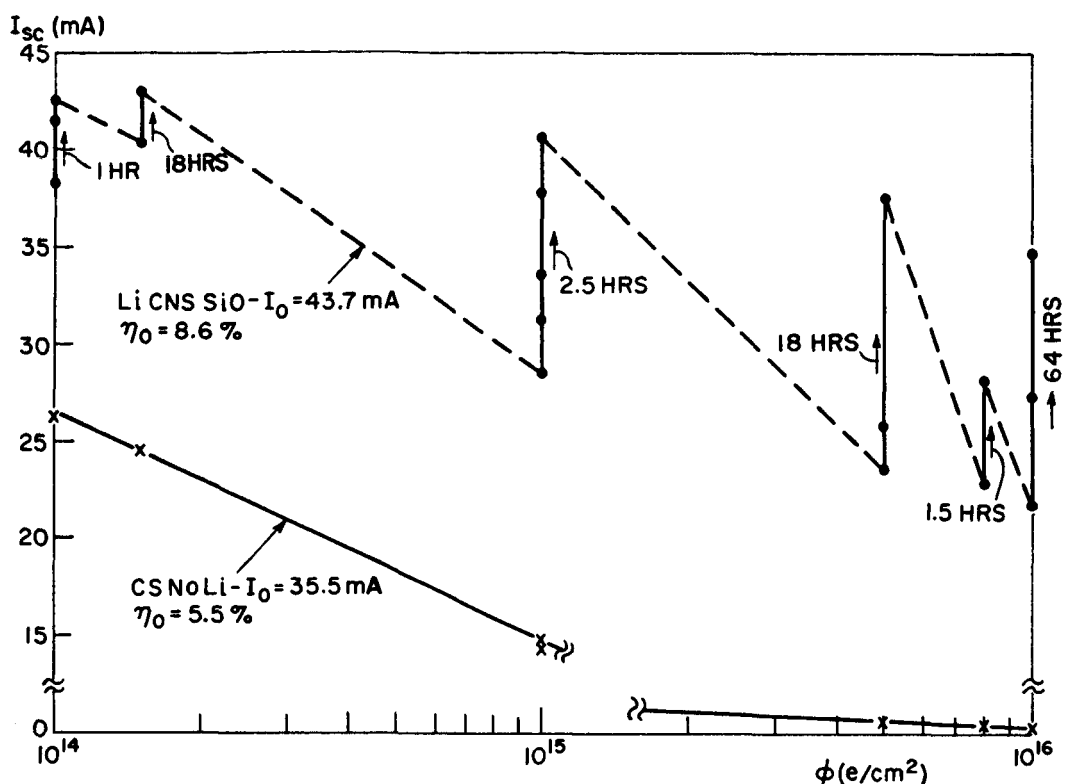


Fig. 17. Short-circuit current as a function of irradiation.

current  $I_{sc}$  measured in filtered incandescent light also recovered when the bombardment is stopped. The same behavior was observed in the maximum power output  $P_{max}$ , as shown in Fig. 18. The lithium-doped cell was initially 8.6% efficient; when allowed to recover for 112 hours after  $1 \times 10^{16} \text{ e/cm}^2$  (a flux which reduces the standard cell's efficiency essentially to zero), its efficiency was still 6.6%!

Because the bombardment *rate* is an important factor in the observed behavior of these cells, an experiment was performed at two different rates to compare a lithium-diffused cell with commercial Q.C. n/p and p/n cells. The bombardment rate was  $\approx 5 \times 10^{12} \text{ e/cm}^2/\text{hr}$  to  $1 \times 10^{14} \text{ e/cm}^2/\text{hr}$ , a rate which is considerably higher than that commonly observed in space satellites. Continued irradiation at the low rate was impracticable in terms of machine time, so that the rate was increased by a factor of 100. Figure 19 shows how  $P_{max}$  varied as a function of  $\phi$ . Very little change occurred in either the lithium-diffused or the n/p cell up to  $1 \times 10^{14} \text{ e/cm}^2$ . At the higher irradiation rate and fluxes, however,  $P_{max}$  in the lithium-doped cell fell below that of the n/p cell, but it recovered over the weekend to exceed the performance of the n/p cell! At rates of  $5 \times 10^{12} \text{ e/cm}^2/\text{hr}$  or below, lithium apparently has sufficient time to interact with the induced damage centers. The damage centers are introduced too rapidly at the high rate, however, and lithium cannot diffuse fast enough to neutralize them. (This recovery would be expected to accelerate as the cell temperature was increased.) This experiment suggests the lithium-diffused cell, if irradiated slowly enough (for example, at rates found in space), would exceed the n/p cell in radiation resistance even during radiation.

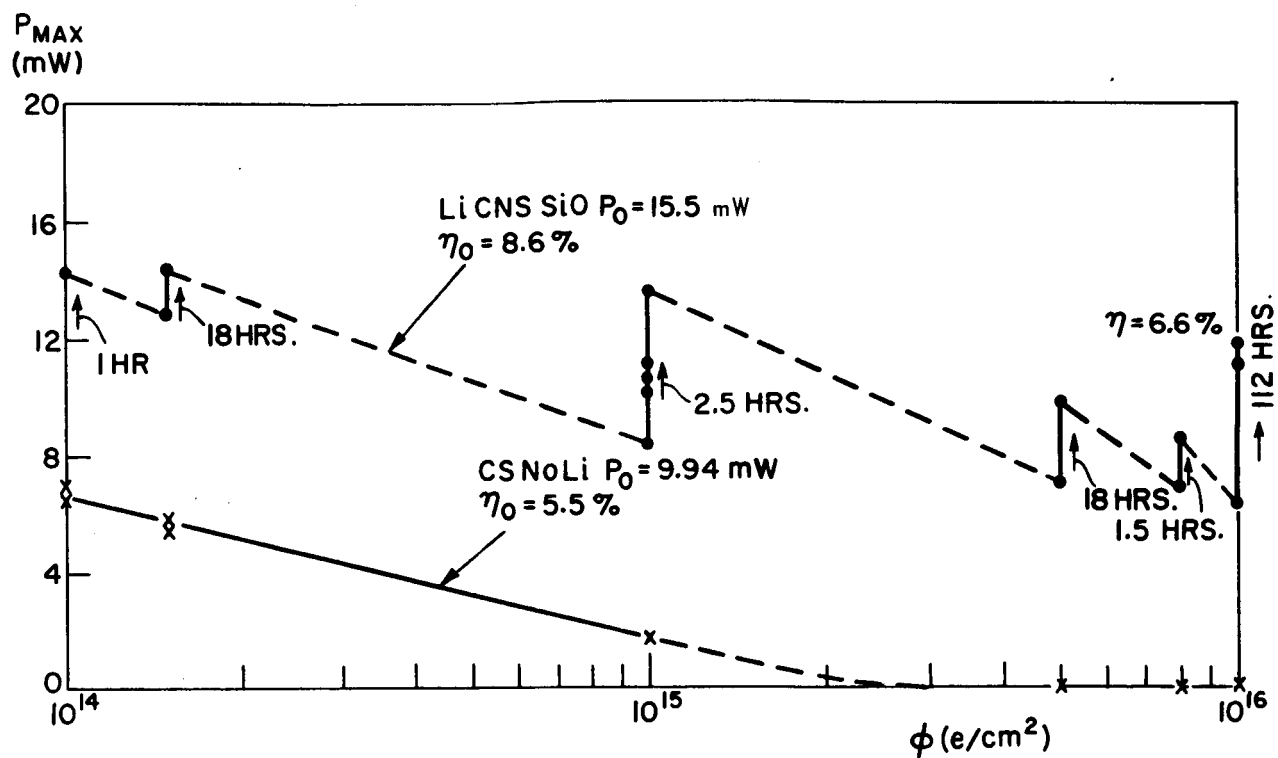


Fig. 18. Maximum power output as a function of irradiation.

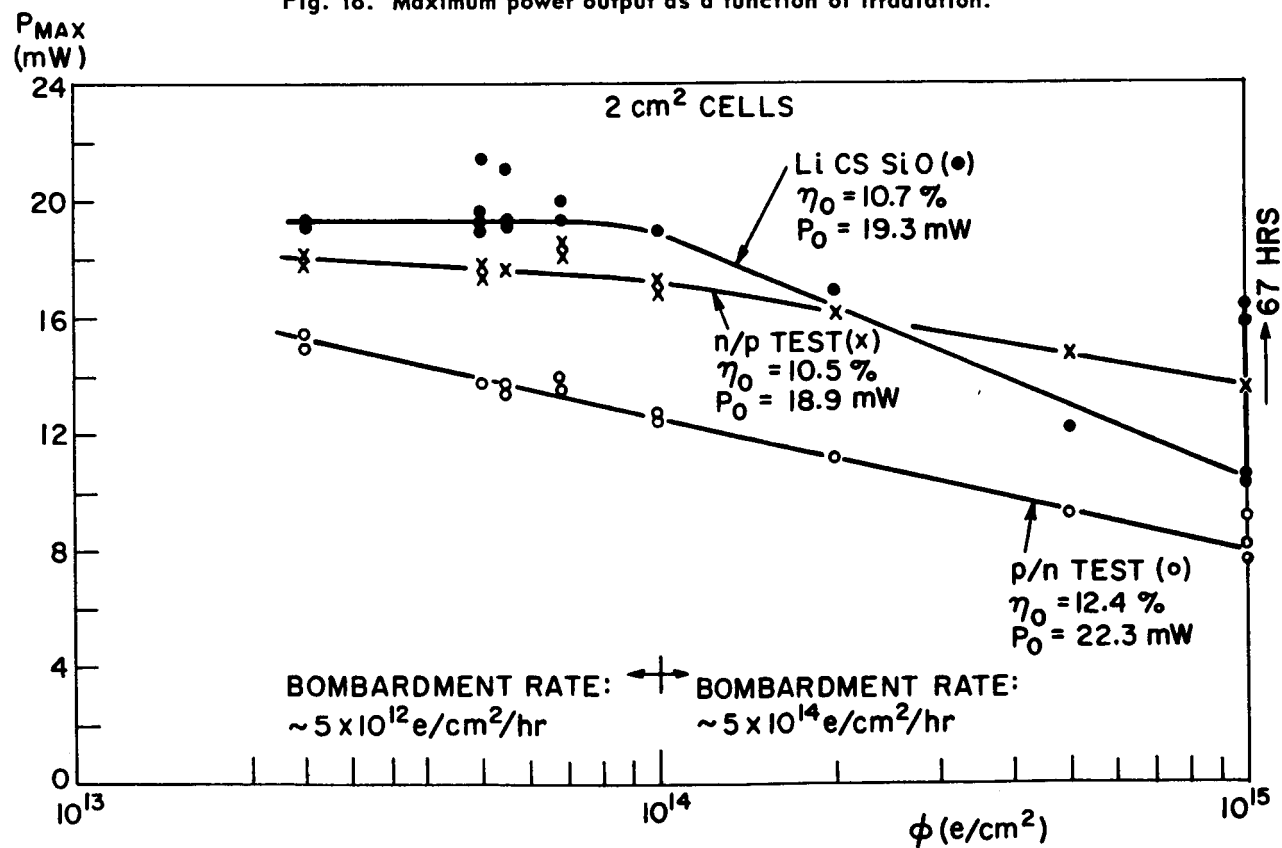


Fig. 19. Maximum power output as a function of flux.

Table I summarizes the electrical performance of these cells in both filtered incandescent light and in sunlight.

TABLE I  
COMPARISON OF  $1 \times 2$  cm SOLAR CELLS

| CELL                        | INITIAL-<br>SUNLIGHT |               | FILTERED INCANDESCENT LIGHT                      |               |   |               |                  |               | AFTER 2 DAYS<br>SUNLIGHT |               |
|-----------------------------|----------------------|---------------|--|---------------|---|---------------|------------------|---------------|--------------------------|---------------|
|                             |                      |               | $1 \times 10^{14}$ e/cm <sup>2</sup><br>Low Rate |               | $1 \times 10^{15}$ e/cm <sup>2</sup><br>High Rate |               | After 2<br>Days  |               |                          |               |
|                             | $I_{sc}$<br>(mA)     | $\eta$<br>(%) | $I_{sc}$<br>(mA)                                 | $\eta$<br>(%) | $I_{sc}$<br>(mA)                                  | $\eta$<br>(%) | $I_{sc}$<br>(mA) | $\eta$<br>(%) | $I_{sc}$<br>(mA)         | $\eta$<br>(%) |
|                             | Li p/n               | 51            | 10.7   | 49.3          | 10.5  | 33            | 5.8              | 47            | 8.9                      | 47            |
| n/p; $\approx 2 \Omega$ -cm | 56.4                 | 10.5          | 50.3   | 9.6           | 40  | 7.6           | 40               | 7.7           | 42                       | 7.5           |
| p/n; $\approx 2 \Omega$ -cm | 60.3                 | 12.4          | 34.8   | 7.0           | 24  | 4.4           | 24.3             | 4.6           | 28.3                     | 5.1           |

The spectral response data of the above cells are shown in Figs. 20 and 21. The n/p cell is not shown since its behavior was qualitatively similar to the behavior of the p/n cell. The spectral response of the lithium-diffused cell (Fig. 20) did not change at the slow bombardment rate up to a flux of  $6.8 \times 10^{13}$  e/cm<sup>2</sup>. After the high-rate bombardment of  $1 \times 10^{15}$  e/cm<sup>2</sup>, a significant loss in red response occurred, but the red response recovered with time, as shown.

N.R.

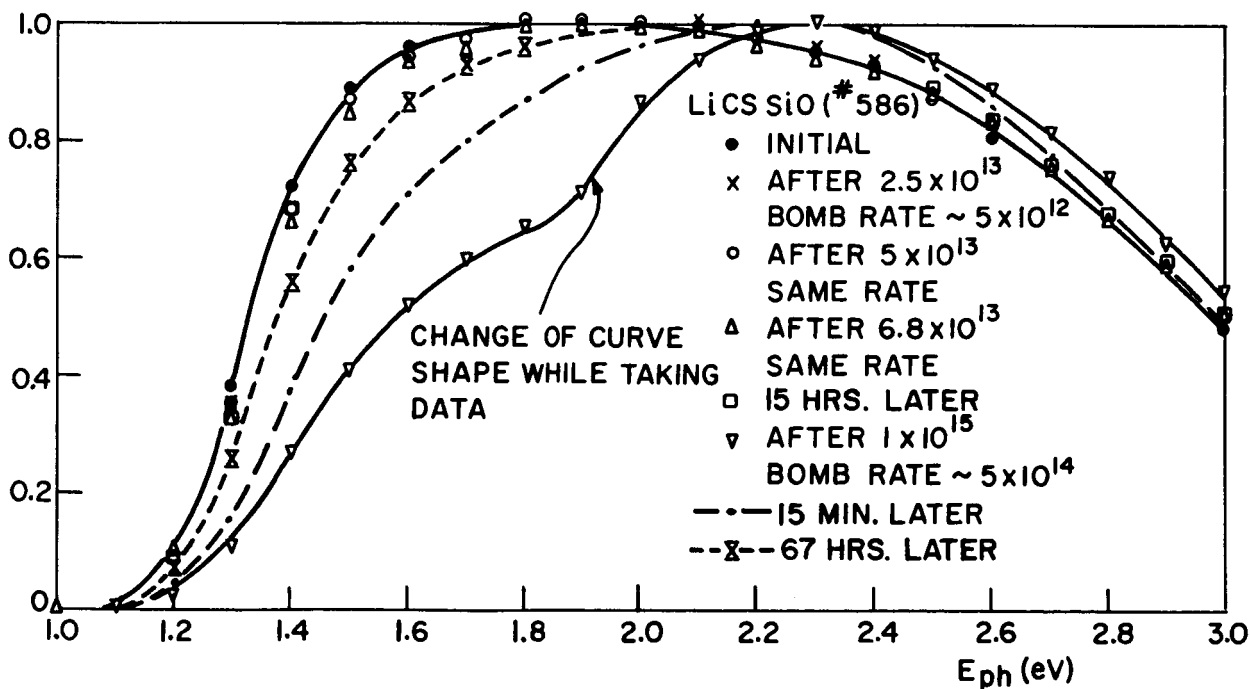


Fig. 20. Spectral response of  $1\text{-cm} \times 2\text{-cm}$  solar cell (LiCS SiO-586).

The slight change of shape in the curve for  $1 \times 10^{15} \text{ e/cm}^2$  is not considered significant; it was probably due to an instrumental effect. The p/n-cell (Fig. 21) behaved as expected; its red response decreased with bombardment and in no instance did it recover.

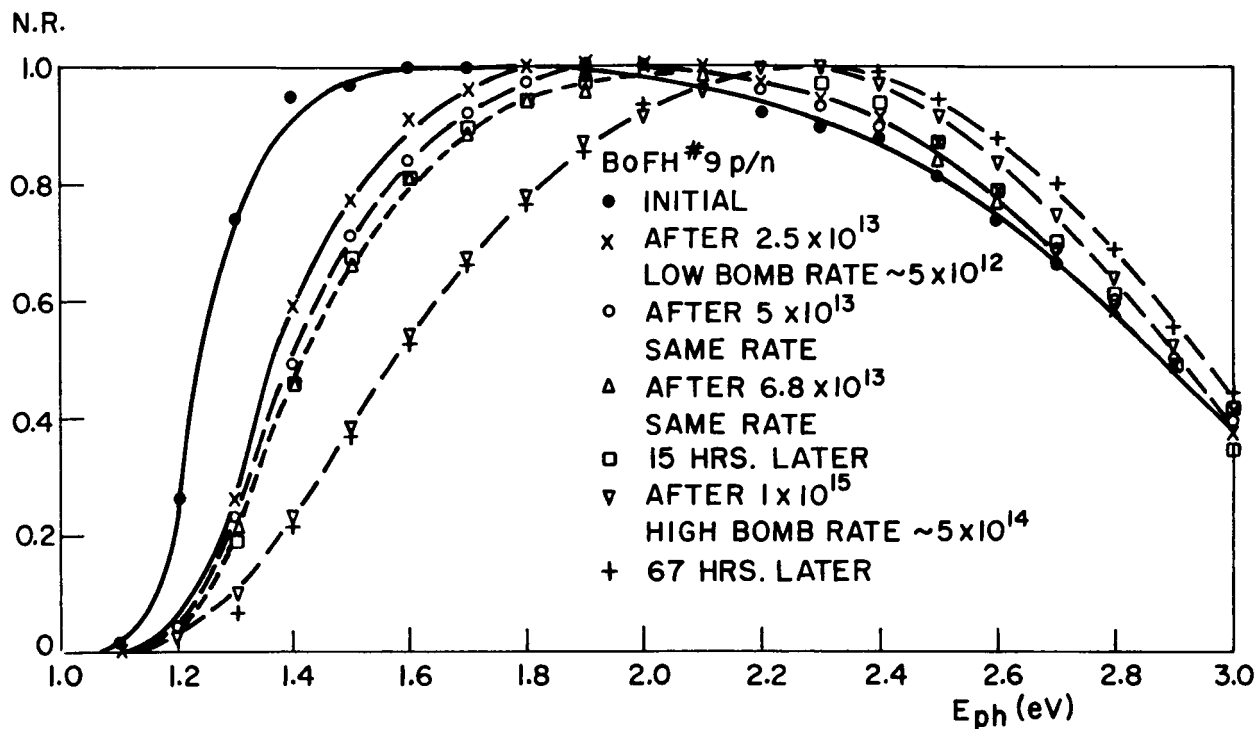


Fig. 21. Spectral response of 1-cm  $\times$  2-cm solar cell (BoFH 9 p/n).

Further evidence for a lithium-damage-center interaction was obtained in isochronal annealing studies. The results of one study involving a lithium-diffused and a standard cell irradiated with a flux of  $10^{16} \text{ e/cm}^2$  is shown in Fig. 22. The fraction of damage  $f$  remaining in  $I_{sc}$  after 10-minute isochronal anneals is plotted against temperature. A reverse-annealing stage centered at  $\approx 75^\circ\text{C}$  occurs in the lithium-diffused cell and not in the standard cell. Such a stage has not been observed before in annealing studies of electron-irradiated solar cells. Therefore, it is inferred that this stage is due to a new center whose temperature stability is not as great as that of previously studied centers. Also noteworthy is that both cells anneal in the same fashion above  $\approx 100^\circ\text{C}$ . (Since some damage is still apparent at  $225^\circ\text{C}$  a higher-temperature annealing stage may also exist.) This behavior of the cells suggests that the residual damage is similar in both. Based on published annealing studies,<sup>15</sup> one is tempted to identify the residual damage in part with the E-center. This identification suggests one model for the lithium-damage-center interaction. Irradiation produces vacancies which are trapped by substitutional phosphorus atoms. Lithium diffuses to, and pairs with, some of these negatively charged centers, reducing their recombination cross sections. Any unpaired centers result in residual damage. The new Li-E-center complex has a low binding energy, so that it breaks up at temperatures around  $75^\circ\text{C}$ , lithium diffusing away, with consequent increased damage due to the increased number of unpaired E-centers. Above  $100^\circ\text{C}$ , the E-center itself breaks up; the vacancy diffuses away and is annihilated, and the residual damage is annealed. This model and others are discussed more fully below.

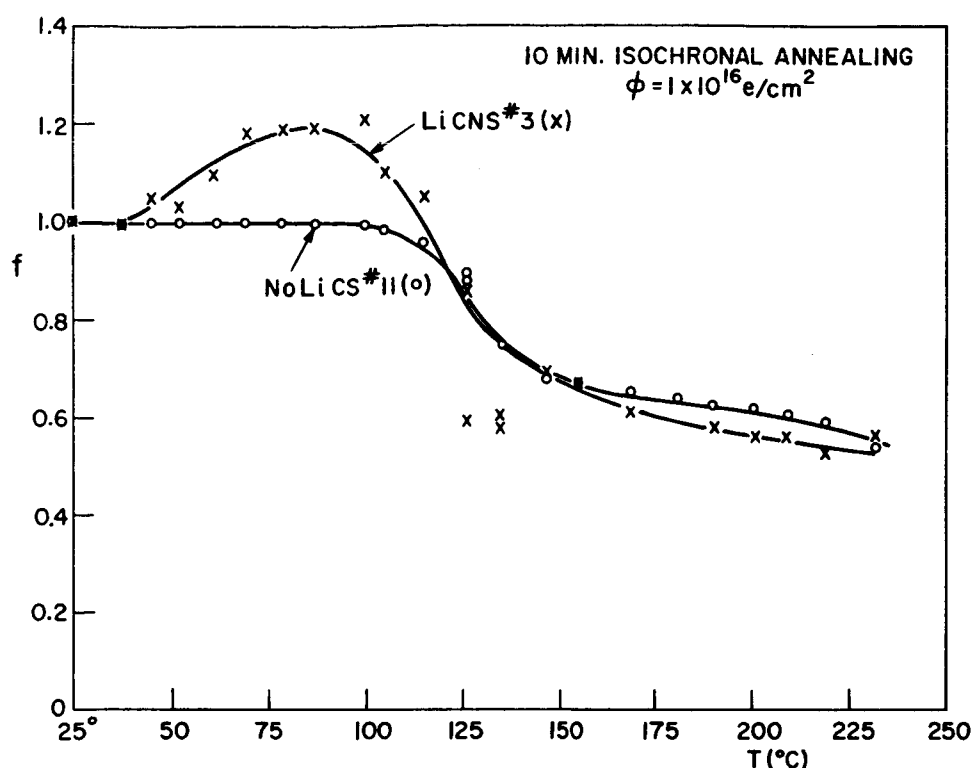


Fig. 22.  
 Fraction of remaining damage (f) as a function of temperature.

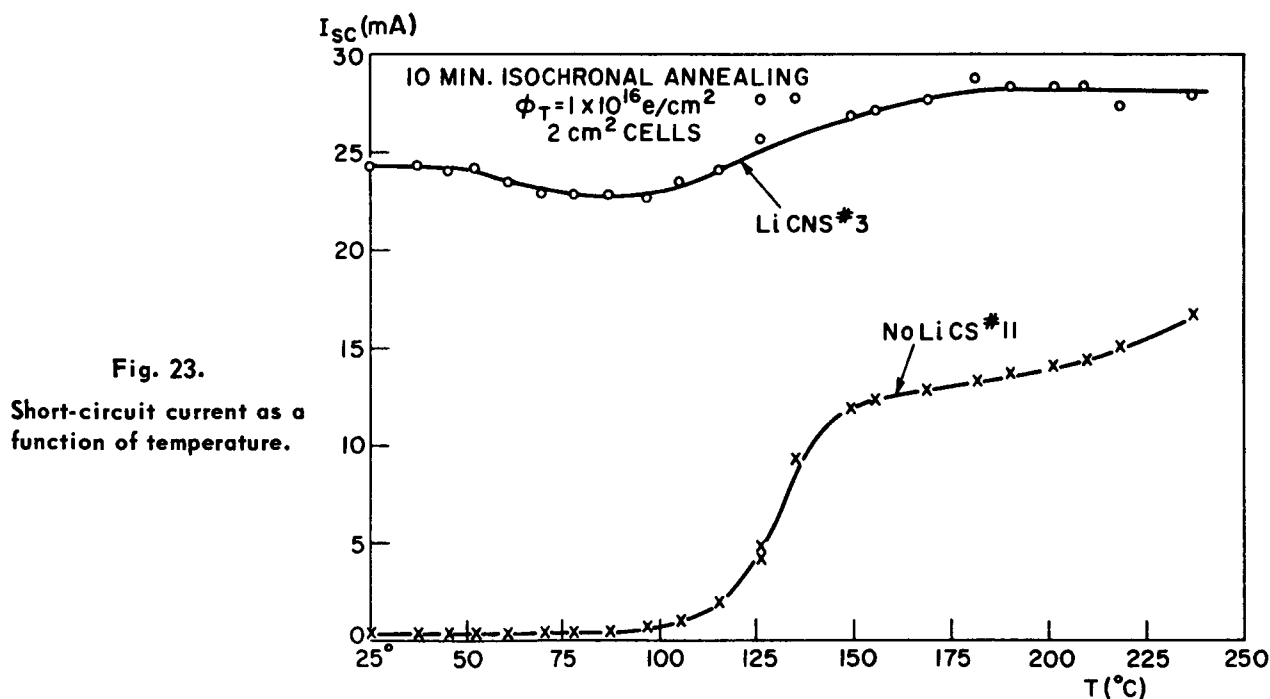


Fig. 23.  
 Short-circuit current as a function of temperature.

It must be emphasized that the reverse-annealing damage in the lithium-diffused cell was not large enough to affect its relative superiority over the standard cell. This fact is demonstrated in Fig. 23 where the actual short-circuit current, instead of the fraction damage left, is plotted. It is apparent that the performance of the lithium-diffused cell far exceeds that of the standard cell even considering the reverse-annealing damage.



Isothermal annealing measurements were also made to determine the activation energy for annealing of the defects involved. The results of one such measurement at 80°C is shown in Fig. 24. Although the reverse-annealing stage of the lithium-doped cell is seen to occur, the cell recovers from even this damage during the periods of the experiment in which the cell was at room temperature. The vertical arrows near the data show the direction of this recovery. No such behavior was seen in the standard cell. The scatter resulting from the behavior of the lithium-diffused cell unfortunately made subsequent analysis for the activation energy for annealing of the defect impossible.

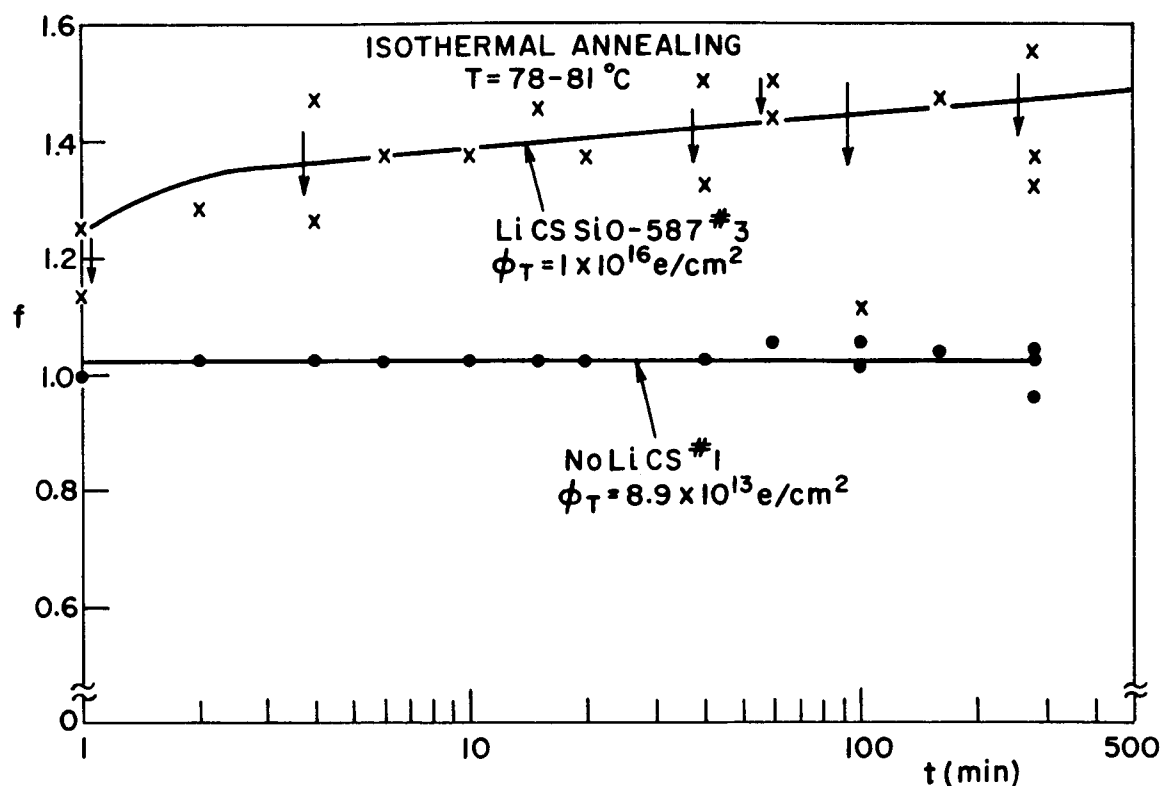


Fig. 24. Isothermal annealing measurements.

## 2. Proton Irradiations

Lithium-diffused and standard p/n cells were compared with commercial Q.C. p/n and n/p cells in a 16.8-MeV proton irradiation. Sufficient time was not available to reduce and analyze the data, including establishing the flux scale, at the time of this report, but comparative data obtained with a filtered incandescent light can be given.

The initial values of the various cell properties are listed in Table II. The photovoltaic outputs were measured in sunlight. Most of the cells had a high conversion efficiency, and approximately the same resistivity in the vicinity of the junction, with the exception of the standard p/n cells.

TABLE II  
INITIAL CELL PROPERTIES

| PROPERTY                            | Li p/n   | STD. p/n  | COM. p/n  | COM. n/p  |
|-------------------------------------|----------|-----------|-----------|-----------|
| $\rho^*$ ( $\Omega$ -cm)            | 2-5      | 11-12     | 0.3-1.8   | 1.8-2.3   |
| $J_s$ (mA/cm <sup>2</sup> )         | 26-32.2  | 27.2-30.4 | 28.4-30.2 | 30.2-32.0 |
| Average $J_s$ (mA/cm <sup>2</sup> ) | 30.2     | 29.1      | 28.9      | 31.2      |
| $\eta$ (%)                          | 5.8-12.1 | 6.8-9.6   | 11-12.6   | 11.8-12.8 |
| Average $\eta$ (%)                  | 9.1      | 8.2       | 11.8      | 12.3      |

\*In vicinity of junction as deduced from capacitance measurements.

The fractional change in  $I_{sc}$  and  $P_{max}$  are shown in Figs. 25 and 26 as a function of flux. Both figures show the standard p/n cells to be surprisingly radiation-resistant, certainly due in part to their higher base resistivity, and show that the lithium-doped cells immediately after irradiation are comparable in performance to the n/p cells. The commercial p/n cells are inferior to the other cells. The lithium-doped cells began to recover after irradiation and the figures show the remarkable recovery of these cells in ten days. No other cell showed such recovery. It is evident that lithium also interacts with proton-induced damage in a fashion that is similar to the electron-bombarded case. A low bombardment rate may thus result in almost no damage to the lithium cells at levels of even  $5 \times 10^{11}$  p/cm<sup>2</sup>.

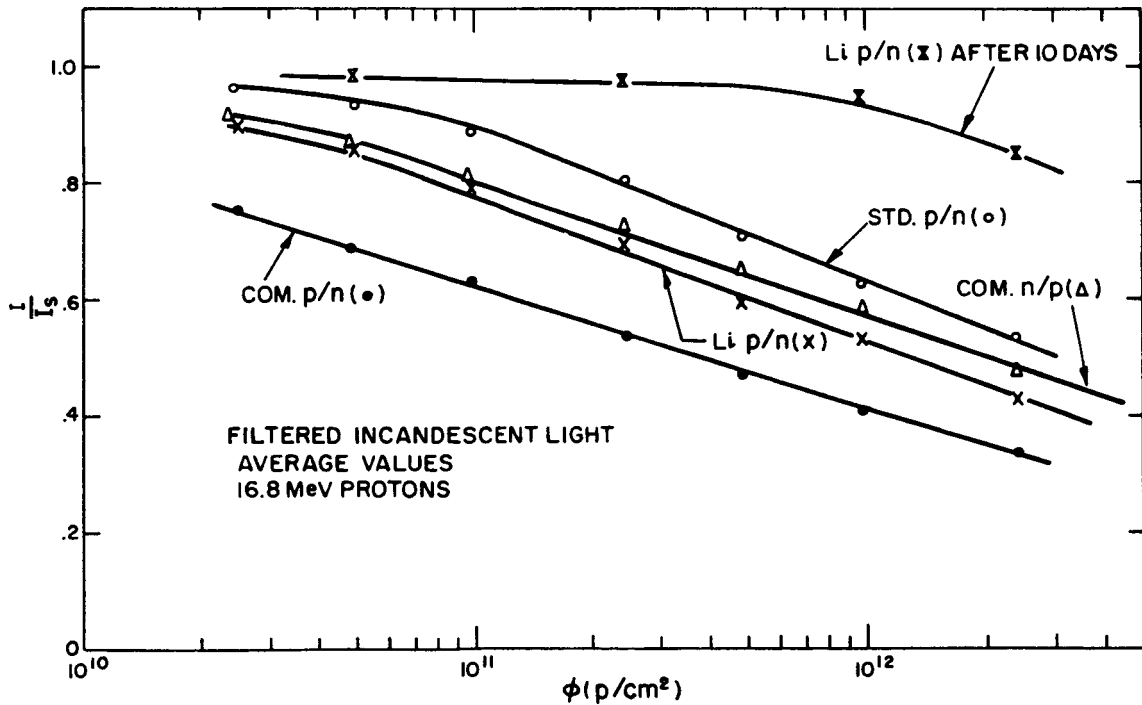


Fig. 25.  $I_{sc}$  as a function of flux of 16-MeV protons.

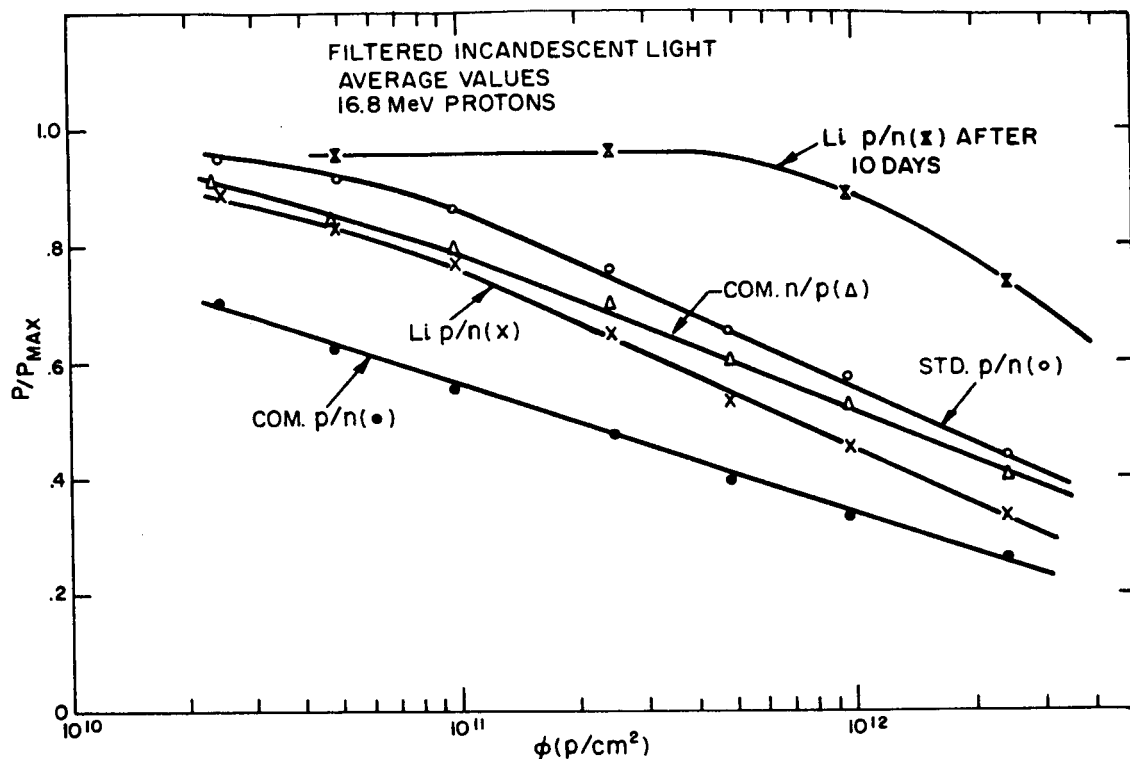


Fig. 26.  $P_{max}$  as a function of flux of 16.8-MeV protons.

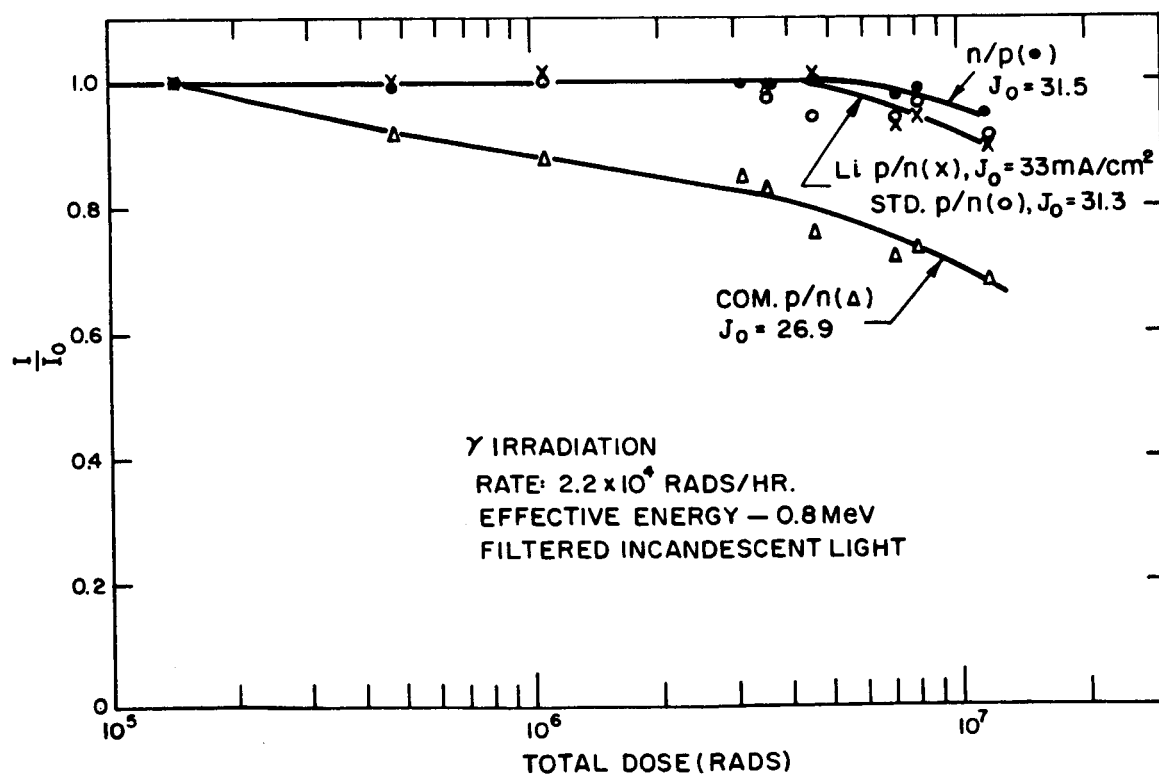


Fig. 27. Fractional change in current vs. gamma dose.

### 3. Gamma Irradiations

A low-level gamma irradiation was started in order to confirm whether or not lithium-diffused cells will be superior to n/p cells if irradiated slowly. The gamma source is a spent fission element located at the Industrial Reactor Laboratory, Plainsboro, N. J. The effective gamma energy is 0.8 MeV, and the dose rate is  $2.2 \times 10^4$  rads/hour.

The fractional change in  $I_{sc}$  measured in filtered incandescent light is shown in Fig. 27 for the four cells in the test. The commercial p/n cell is clearly inferior to the other three cells. The other data cluster together, but there is a suggestion that the n/p cell is somewhat better than either the lithium-diffused or the standard cell. Other experiments at higher dose rates are planned to see if the behavior of the lithium-doped cell is possibly different under gamma irradiation.

### E. DISCUSSION

Lithium has been found to have a profound and beneficial effect on the damage behavior of F.Z. p/n solar cells. The question arises as to the mechanism through which this effect occurs. To be comprehensive, any model of the lithium-damage interaction must explain the following salient features of the experimental results.

1. The annealing behavior of oxygen-containing cells is modified by the presence of lithium in concentrations comparable to the existing phosphorus concentration. The modification consists of the presence of a prominent annealing stage at  $\approx 100^\circ\text{C}$  which is not found in similar cells which do not contain lithium.
2. The electron- and photo-voltaic response of F.Z. cells in which the lithium concentration exceeded the existing phosphorus concentration degraded only slightly where irradiated at a low rate. At a high irradiation rate, the response of the lithium cells degraded during bombardment at a rate very similar to that found in cells made from the same material without lithium.
3. The diffusion length, spectral response, short-circuit current and maximum power output of the lithium cells recovered by a substantial amount from the damage introduced at a high rate by energetic electrons and protons. The residual damage in the lithium cells after recovery was much less than that found in similar cells which did not contain lithium.
4. The time constant for the recovery of the diffusion length in the lithium cells after a high-rate bombardment increased with flux. The recovery time constant was apparently inversely proportional to the diffusion constant of lithium.
5. A reverse-annealing stage at  $\approx 75^\circ\text{C}$  occurred in the bombarded lithium cells. When the temperature was reduced to room temperature, however, the lithium cells subsequently recovered from the reverse-annealing damage.
6. An annealing stage occurred at  $\approx 100^\circ\text{C}$  which was qualitatively similar in both the lithium cell and the one made from the same material without lithium. Since some of the damage remained at  $\approx 225^\circ\text{C}$ , another higher-temperature annealing stage may exist in both cells.

7. Despite the qualitative similarity in annealing, the magnitude of the damage which remained at any temperature was much less in the lithium cell than in the undoped cell.

Of all these results, item 1 is the easiest to explain. It is well-known that lithium pairs with oxygen in silicon.<sup>12</sup> This pairing reduces the amount of oxygen available for subsequent interaction with radiation-induced vacancies. As a result, the vacancies pair with phosphorus to form E-centers. The degradation of the lithium-doped and undoped cells is comparable because the introduction rates of the E- and the A-center are comparable. The E- and the A-centers, however, anneal at different temperatures, namely  $\approx 100^\circ\text{C}$  and  $\approx 250^\circ\text{C}$ , respectively. This model is consistent with the results obtained in these experiments, as well as with spin-resonance work on similar material, discussed in Section II, and with published studies.<sup>16,17</sup>

The other items are not as easily understood at this time, but a model can be developed which is consistent with them. These results are certainly manifestations of a new interaction with radiation-induced defects, i.e., a new center involving lithium. The formation of this center concerns us here.

The model which is proposed postulates that lithium interacts with a defect which is immobile at room temperature. At least two such defects are known in n-type, F.Z. silicon, namely the divacancy (C-center) and the E-center. Both of these centers can be formed in the material used in this study because the C-center is an intrinsic defect, and because some phosphorus ( $\approx 2$  to  $4 \times 10^{14}/\text{cm}^3$ ) is present for the formation of the E-center. In the proposed model, the new center is formed in the following fashion. Radiation induces divacancies, and vacancies which complex with each other or with phosphorus to form C- and E-centers. Lithium, in time, diffuses to and pairs with these negatively charged centers to form a new entity or center which may be either a lithium-E, a lithium-C, or some other complex formed from the preceding two; e.g., a lithium-vacancy center. The experimental results indicate that both the C- and E-centers form. The divacancy cannot be the sole immobile defect because its direct introduction rate is too low at 1 MeV\* and because it is stable<sup>18</sup> at temperatures up to  $300^\circ\text{C}$ , and, hence, would be unable to account for an annealing stage at  $100^\circ\text{C}$ . The E-center, on the other hand, must be another of the defects which is involved because of its high introduction rate and its ability to anneal at  $100^\circ\text{C}$ .

The new center is postulated to be ineffective in the recombination of minority carriers. In a low-rate bombardment, it forms when lithium moves to the immobile C- and E-centers. High bombardment rates create a nonequilibrium situation because the lithium does not diffuse fast enough to interact with the immobile defects. Since these defects are not "neutralized," the lithium-doped cell in this state behaves like an undoped cell made from similar material. The nonequilibrium situation is corrected in time, however, by the pairing of lithium with the immobile defect, resulting in a recovery of the lithium-doped cell, after the cessation of the electron bombardment.

The stability of this new center is such that it breaks up at  $\approx 75^\circ\text{C}$  with the motion of lithium away from the immobile defects. The subsequent recovery at room temperature is due to

\*The possibility exists, of course, that its indirect rate, i.e., the combination of two vacancies, may be high in this material; see Section I-B.

the re-pairing of lithium with the immobile defects. Since the new defects dissociate at 75°C and above, it is expected that the high-temperature annealing in the lithium-doped and the undoped cells will be qualitatively similar because the residual damage is then in effect the same in both cells; i.e., E- and C- centers.

The model involving an initial immobilization of the vacancy and a subsequent pairing interaction with lithium appears to best fit the experimental results given here. Whether the pairing results in a Li-E-center, a Li-C-center, or some other combination such as a lithium-vacancy, must be decided by a quantitative comparison of the damage in the lithium-doped and undoped cells made from similar material, as well as by spin-resonance studies. A quantitative comparison shows that the residual damage in the lithium-doped cell, even during the reverse-annealing stage was always much less than that in the untreated cell. One must argue then, that the pairing results in a center which may not simply be a lithium-E or a lithium-C-center but some other combination such as a lithium-vacancy center. The E- and C-centers would then serve only as catalysts which immobilize the vacancy and promote its reaction with the lithium. Such an interpretation would then be in agreement with the spin-resonance measurements reported elsewhere in which a new spectrum is seen together with the resonance spectrum of phosphorus as a donor; not the slightest trace of any E- or C-centers were observed in the measurement.

It might be argued that an immobile defect is not initially required in the formation of the new center if the end result of the interaction is simply a lithium-vacancy complex. The experimentally observed behavior of the lithium cells, including the bombardment rate and recovery effects, would be very difficult to understand, however, if it is assumed that the new center is a lithium-vacancy complex *and* that it is formed directly during irradiation without any intermediate steps. The reason for this is that while the solar cell recovery time is on the order of hours, the Li-vacancy, if formed directly, should form almost instantaneously since both lithium and vacancies are mobile, and the negatively charged vacancy<sup>19</sup> should pair readily with the positively charged lithium. Hence, a model postulating the direct interaction of lithium and vacancies during irradiation without any intermediate steps is not likely.

It is obvious that more experimental work is required to explain what occurs in lithium-doped cells during irradiation.

## IV. SUMMARY OF CONCLUSIONS AND RECOMMENDATIONS FOR FUTURE WORK

### A. THE K-CENTER

The basic properties of the K-center, the dominant center produced by electron irradiation in p-type silicon, have been well established. The center is formed by a complex of vacancies and oxygen atoms. It is, in its "normal state", a hole trap and it has an energy level 0.3 eV above the valence band. Preliminary measurements have indicated a reverse-annealing at about 250°C, followed by normal annealing of the damage to very low levels by 450°C. A physical model for the K-center, based on a variety of experimental results, is offered in terms of a complex of two vacancies and two oxygen atoms which have trapped a hole.

Future experimental work should center on the very interesting annealing behavior. The details of the reverse-annealing reported here should be studied. The kinetics, activation energy, and if possible the mechanism of the annealing should be elucidated. Other means, such as optical measurements, in addition to electrical and EPR measurements should be employed if found necessary and practicable.

### B. LITHIUM-DEFECT INTERACTIONS

The discovery of strong lithium-defect interactions and their pronounced effects on solar cells and EPR spectra open an extremely fertile field of research. In this section we will summarize briefly some of our findings and suggest future experiments that will, hopefully, further clarify the physics of these interactions and perhaps enhance even more the beneficial effects we have observed in solar cell performance.

#### 1. EPR Studies

The EPR experiments have shown directly that when lithium is the dominant dopant in n-type silicon, exceeding by far the oxygen and phosphorus concentrations, lithium-damage center interactions readily occur. By directly we mean the observation of a new paramagnetic center which is present only when both lithium and damage centers are present in the silicon. This new center, the L-center, has an introduction rate of approximately 0.5/cm. It does not involve phosphorus or oxygen, although these impurities may be involved in the mechanism of the L-center's formation. Certainly the effect of the concentration of these impurities on L-center formation should be studied in the future. This should be quite easy to do since both have their own identifiable paramagnetic resonance. Also, L-center introduction rates should be measured as functions of the various impurity concentrations and bombardment flux levels.

The L-center resonance consists of one line with no discernible angular dependence. It produces an electrical level that is quite shallow, probably 0.03 – 0.06 eV below the conduction band. The binding energy of the L-center must be quite low, since it decreases spontaneously at room temperature and anneals very rapidly at temperatures as low as 80°C. These annealing

experiments should be pursued in the future by both EPR and resistivity measurements. If possible, activation and binding energies should be determined by isochronal and isothermal measurements.

At this time, the two major questions to be answered should be (1) what does the L-center consist of, and (2) what, if any, connection exists between the lithium-damage-center interactions as measured by EPR and the effects of lithium on a solar cell's radiation resistance?

## 2. Increased Radiation Resistance of Solar Cells

Solar cells made from n-type F.Z. silicon in which the predominant dopant is lithium have a much greater radiation-resistance to electrons and protons than ordinary commercial cells. This resistance takes two forms. The first is a post-irradiation recovery in a time of several hours; the recovery is almost complete for low flux levels and is substantial for higher flux levels; in all cases the degradation remaining in lithium cells at a given time after the irradiation is much less than in cells with no lithium. The second is a much lower degradation rate during bombardment of lithium-containing cells than is currently found for cells which do not contain lithium, when the bombardment rate is low. *If the bombardment rate is sufficiently low (but still higher than that expected in space) hardly any degradation is observed in the lithium-containing cells.* Obviously, if the flux rates are low enough, recovery can occur during the irradiation so that no degradation, in effect, takes place.

Several experiments should be performed in the future as "follow-up" to the effects described above using junction and/or solar cell properties as measurement parameters. The recovery behavior at different temperatures, after irradiations at different flux levels and flux rates, should be studied. The annealing behavior should be investigated over a wider temperature range. The dependence of the recovery behavior on the phosphorus and oxygen concentrations relative to the lithium concentration should also be studied with the aim of clarifying the mechanism of the lithium interactions.

Many of the experiments suggested above have their parallel in EPR studies and should, if possible, be so performed that a consistent picture ultimately emerges.

In the solar cell area, we consider that the most important experimental approach is one that is directed toward (1) enhancing even further the radiation-resistance due to lithium already found, and (2) a clarification of the detailed mechanism of the role played by lithium.

A very important question concerns the long-term reliability of these cells. Any device containing a mobile impurity such as lithium might lose the impurity to surfaces and/or contacts or p/n junction regions. Furthermore, this effect might be accelerated at elevated temperatures at which some space vehicles operate. Therefore, shelf life and operating life under varying conditions exclusive of particle radiation should be determined.



## REFERENCES

1. V. S. Vavilov and A. F. Plotnikov, J. Phys. Soc. Japan **18**, 30 (1963).
2. H. Y. Fan and A. K. Ramdas, J. Appl. Phys. **30**, 1127 (1959).
3. G. D. Watkins, J. Phys. Soc., Japan **18**, 22 (1963).
4. H. Reiss and W. Kaiser, *Properties of Elemental and Compound Semiconductors* (Interscience Publishers, New York, 1960).
5. G. D. Watkins and J. W. Corbett, Disc. Far. Soc. **31**, 86 (1961).
6. P. Fang, Phys. Letters **20**, 343 (1966).
7. B. Goldstein, N. Almeleh, and J. Wysocki, Final Report, Contract No. NAS 5-9131 (1965).
8. J. Corbett and G. Watkins, Phys. Rev. **138**, A555 (1965).
9. G. Ludwig and H. Woodbury, Solid State Physics **13**, 279 (1962).
10. W. Rosenzweig, Bell System Tech. J. **41**, 1573 (1962).
11. H. Reiss, et al., Bell Syst. Tech. J. **35**, 535 (1956).
12. E. M. Pell, *Solid State Physics in Electronics and Telecommunications*, Ed. by M. Desirant and J. L. Michiels, Vol. 1, Part 1 (Academic Press, New York, 1960).
13. W. Kaiser and P. Keck, J. Appl. Phys. **28**, 882 (1957).
14. R. Logan and A. Peters, J. Appl. Phys. **30**, 1627 (1959).
15. E. Sonder and L. Templeton, J. Appl. Phys. **34**, 3295 (1963).
16. V. Vavilov, et al., Soviet Physics-Solid State **4**, 830 (1962).
17. V. Vavilov, et al., Soviet Physics-Solid State **6**, 2097 (1965).
18. G. Watkins and J. Corbett, Phys. Rev. **138**, A 543 (1965).
19. G. Watkins, *Proceedings of the Symposium on Radiation Damage in Semiconductors*, Paris 1964 (Dunod Cie, Paris 1965).